MitoEAGLE preprint 2017-09-21

2017-09-21 preprint version 01

The protonmotive force and respiratory control: Building blocks of mitochondrial physiology Part 1.

MitoEAGLE Network

Corresponding author: Gnaiger E

Contributing co-authors (*alphabetical, to be extended*):

Ahn B, Alves MG, Beard DA, Ben-Shachar D, Bishop D, Breton S, Brown GC, Brown RA, Buettner GR, Cervinkova Z, Chicco AJ, Coen PM, Collins JL, Crisóstomo L, Davis MS, Dias T, Doerrier C, Ehinger J, Elmer E, Fell DA, Filipovska A, Garcia-Roves PM, Garcia-Souza LF, Genova ML, Gonzalo H, Goodpaster BH, Han J, Harrison DK, Hellgren KT, Hernansanz P, Hoppel CL, Iglesias-Gonzalez J, Irving BA, Iyer S, Jansen-Dürr P, Jespersen NR, Jha RK, Käämbre T, Kane DA, Kappler L, Keijer J, Komlodi T, Kuang J, Labieniec-Watala M, Laner V, Lee HK, Lemieux H, Lerfall J, Lucchinetti E, Makrecka-Kuka M, Meszaros AT, Moisoi N, Molina AJA, Montaigne D, Moore AL, Murray AJ, Nozickova K, Oliveira PF, Oliveira PJ, Orynbayeva Z, Palmeira CM, Patel HH, Pesta D, Petit PX, Pichaud N, Pirkmajer S, Porter RK, Pranger F, Prochownik EV, Reboredo P, Renner-Sattler K, Rohlena J, Røsland GV, Rossiter HB, Salvadego D, Scatena R, Schartner M, Scheibye-Knudsen M, Schilling JM, Schlattner U, Schoenfeld P, Scott GR, Singer D, Sobotka O, Spinazzi M, Stocker R, Sumbalova Z, Suravajhala P, Tanaka M, Tandler B, Tepp K, Towheed A, Trivigno C, Tronstad KJ, Tyrrell DJ, Velika B, Vendelin M, Vercesi AE, Ward ML, Watala C, Wei YH, Wieckowski MR, Wolff J, Wuest RCI, Zaugg M, Zorzano A

Supporting co-authors (*alphabetical*):

Arandarčikaitė O, Bakker BM, Batista Ferreira J, Bernardi P, Boetker HE, Borsheim E, Borutaitė V, Bouitbir J, Calabria E, Calbet JA, Carvalho E, Chaurasia B, Clementi E, Collin A, Das AM, De Palma C, Distefano G, Dubouchaud H, Duchen MR, Durham WJ, Dyrstad SE, Fornaro M, Gan Z, Garlid KD, Garten A, Gourlay CW, Granata C, Haas CB, Haendeler J, Hand SC, Hepple RT, Hickey AJ, Hoel F, Kainulainen H, Keppner G, Khamoui AV, Klingenspor M, Koopman WJH, Kowaltowski AJ, Krajcova A, Lenaz G, MacMillan-Crow LA, Malik A, Markova M, Mazat JP, Menze MA, Methner A, Muntané J, Muntean DM, Neuzil J, Newsom S, O'Gorman D, Oliveira MT, Pak YMK, Pettersen IKN, Pulinilkunnil T, Robinson MM, Ropelle ER, Salin K, Sandi C, Sazanov LA, Siewiera K, Silber AM, Skolik R, Smenes BT, Soares FAA, Sokolova I, Sonkar VK, Stankova P, Swerdlow RH, Szabo I, Thyfault JP, Tretter L, Vieyra A, Votion DM, Williams C, Zaugg K

Updates:

http://www.mitoeagle.org/index.php/MitoEAGLE_preprint_2017-09-21

Correspondence: Gnaiger E
Department of Visceral, Transplant and Thoracic Surgery, D. Swarovski Research Laboratory, Medical University of Innsbruck, Innrain 66/4, A-6020 Innsbruck, Austria
Email: erich.gnaiger@i-med.ac.at
Tel: +43 512 566796, Fax: +43 512 566796 20

This manuscript on 'The protonmotive force and respiratory control' is a position statement in the frame of COST Action CA15203 MitoEAGLE. The list of co-authors evolved from MitoEAGLE Working Group Meetings and a ***bottom-up*** *spirit of COST: This is an open invitation to scientists and students to join as co-authors, to provide a balanced view on mitochondrial respiratory control, a fundamental introductory presentation of the concept of the protonmotive force, and a critical discussion on reporting data of mitochondrial respiration in terms of metabolic flows and fluxes. We plan a series of follow-up reports by the expanding MitoEAGLE Network, to increase the scope of consensus-oriented recommendations and facilitate global communication and collaboration.*

We continue to invite comments and suggestions on the MitoEAGLE preprint (phase 2; until ***October 12****), particularly if you are an* ***early career investigator adding an open future-oriented perspective****, or an* ***established scientist providing a balanced historical basis****. Your critical input into the quality of the manuscript will be most welcome, improving our aims to be educational, general, consensus-oriented, and practically helpful for students working in mitochondrial respiratory physiology.*

Please feel free to focus on a particular section in terms of direct input and references, while evaluating the entire scope of the manuscript from the perspective of your expertise.

Your comments will be largely posted on the discussion page of the MitoEAGLE preprint website. If you prefer to submit comments in the format of a referee's evaluation rather than a contribution as a co-author, I will be glad to distribute your views to the updated list of co-authors for a balanced response. We would ask for your consent on this open bottom-up procedure.

*We organize a MitoEAGLE session linked to our series of reports at the MiP*conference *Nov 2017 in Hradec Kralove in close association with the MiPsociety (where you hopefully will attend) and at EBEC 2018 in Budapest.*

» http://www.mitoeagle.org/index.php/MiP2017_Hradec_Kralove_CZ

I thank you in advance for your feedback.
With best wishes,

Erich Gnaiger
Chair Mitochondrial Physiology Society - http://www.mitophysiology.org
Chair COST Action MitoEAGLE - http://www.mitoeagle.org
Medical University of Innsbruck, Austria

Contents

Abstract

Clarity of concepts and consistency of nomenclature are trademarks of a research field across its specializations, facilitating transdisciplinary communication and education. As research and knowledge of mitochondrial physiology expand, the necessity for harmonizing nomenclature concerning mitochondrial respiratory states and rates has become apparent. Peter Mitchell's concept of the protonmotive force establishes the links between electrical and chemical components of energy transformation and coupling in oxidative phosphorylation. This unifying concept provides the framework for developing a consistent terminology of mitochondrial physiology and bioenergetics. We follow IUPAC guidelines on general terms of physical chemistry, extended by concepts of open systems and irreversible thermodynamics. We align the nomenclature of classical bioenergetics on respiratory states with a concept-driven constructive terminology to address the meaning of each respiratory state. Standards for evaluation of respiratory states must be followed for the development of databases of mitochondrial respiratory function in species, tissues and cells studied under diverse physiological and experimental conditions.

Keywords: Mitochondrial respiratory control, coupling control, mitochondrial preparations, protonmotive force, chemiosmotic theory, oxidative phosphorylation, OXPHOS, efficiency, electron transfer system, ETS; proton leak, LEAK, residual oxygen consumption, ROX, State 2, State 3, State 4, normalization, flow, flux

Box 1: In brief - mitochondria and Bioblasts

* Does the public expect biologists to understand Darwin's theory of evolution?
* Do students expect that researchers of bioenergetics can explain Mitchell's theory of chemiosmotic energy transformation?

Mitochondria are dynamic organelles contained within eukaryotic cells, with a double membrane. The inner mitochondrial membrane shows dynamic tubular and disk-shaped cristae that separate the mitochondrial matrix, *i.e.* the internal mitochondrial compartment, and the intermembrane space; the latter being enclosed by the outer mitochondrial membrane. Mitochondria were described for the first time in 1857 by Rudolph Albert von Kölliker as granular structures or 'sarkosomes'. In 1886 Richard Altman called them 'bioblasts' (published 1894). The word 'mitochondrium' (Greek mitos: thread; chondros: granule) was introduced by Carl Benda (1898). Mitochondria are the oxygen consuming electrochemical generators which evolved from endosymbiotic bacteria (Margulis 1970). The bioblasts of Richard Altmann (1894) include not only the mitochondria as presently defined, but also symbiotic and free-living bacteria. Mitochondria are the structural and functional elemental units of cell respiration, where cell respiration is defined as the consumption of oxygen coupled to electrochemical proton translocation across the inner mitochondrial membrane. In the process of oxidative phosphorylation (OXPHOS), the reduction of O_2 is electrochemically coupled to conservation of energy in the form of ATP (Mitchell 2011). As part of the OXPHOS system, these powerhouses of the cell contain the transmembrane respiratory complexes (i.e. FMN, Fe-S and cytochrome *b*, *c*, aa_3 redox systems), alternative dehydrogenases and oxidases, the coenzyme ubiquinone (Coenzyme Q, CoQ) and ATP synthase together with the enzymes of the tricarboxylic acid cycle and the fatty acid oxidation enzymes, ion transporters, including substrate, co-factor and metabolite transporters as well as proton pumps, and mitochondrial kinases related to energy transfer pathways. The mitochondrial proteome comprises over 1,200 proteins (Mitocharta), mostly encoded by nuclear DNA (nDNA), with a variety of functions,

many of which are relatively well known (*e.g.* apoptosis-regulating proteins), are still under investigation, or need to be identified (alanine transporter). Mitochondria maintain several copies of their own genome (hundred to thousands per cell) which is maternally inherited and known as mitochondrial DNA (mtDNA). mtDNA is 16.5 Kb in length, contains 13 protein-coding genes for subunits of the transmembrane respiratory Complexes CI, CIII, CIV and ATP synthase, and also encodes 22 tRNAs and the mitochondrial 16S and 12S rRNA. The mitochondrial genome is both regulated and supplemented by nuclear-encoded mitochondrial targeted proteins. Evidence has accumulated that additional gene content is encoded in the mitochondrial genome, e.g. microRNAs, smithRNAs, and even additional proteins. The inner mitochondrial membrane contains the non-bilayer phospholipid cardiolipin, which is not present in any other eukaryotic cellular membrane. Cardiolipin promotes the formation of respiratory supercomplexes, which are supramolecular assemblies based upon specific, though dynamic, interactions between individual respiratory complexes (Lenaz *et al.* 2017). There is a constant crosstalk between mitochondria and the other cellular components at the transcriptional or post-translational level, and through cell signalling in response to varying energy demands (Quiros *et al.* 2016). Mitochondrial morphology can change in response to energy requirements of the cell via processes known as fusion and fission through which mitochondria can communicate within a network, and in various pathological states which cause swelling or dysregulation of fission and fusion. Mitochondrial dysfunction is associated with a wide variety of genetic and degenerative diseases. Therefore, a better understanding of mitochondrial physiology will improve our understanding of the etiology of disease and the diagnostic repertoire of mitochondrial medicine. Abbreviation: mt, as generally used in mtDNA. Mitochondrion is singular and mitochondria is plural.

‘*For the physiologist, mitochondria afforded the first opportunity for an experimental approach to structure-function relationships, in particular those involved in active transport,*

vectorial metabolism, and metabolic control mechanisms on a subcellular level' (Ernster and Schatz 1981).

---

1. Introduction

Mitochondria are the powerhouses of the cell with numerous physiological, molecular, and genetic functions (**Box 1**). Every study of mitochondrial function and disease is faced with **E**volution, **A**ge, **G**ender and sex, **L**ifestyle, and **E**nvironment (EAGLE) as essential background conditions characterizing the individual patient or subject, cohort, species, tissue and to some extent even cell line. As a large and highly coordinated group of laboratories and researchers, the global MitoEAGLE Network's mission is to generate the necessary scale, type, and quality of consistent data sets and conditions to address this intrinsic complexity. Harmonization of experimental protocols and implementation of a quality control and data management system is required to interrelate results gathered across a spectrum of studies and to generate a rigorously monitored database focused on mitochondrial respiratory function. In this way, researchers within the same and across different disciplines will be positioned to compare their findings to an agreed upon set of clearly defined and accepted international standards.

Reliability and comparability of quantitative results depend on the accuracy of measurements under strictly-defined conditions. A conceptually clearly-defined framework is also required to warrant meaningful interpretation and comparability of experimental outcomes carried out by research groups at different institutes. With an emphasis on quality of research, collected data can be useful far beyond the specific question of a specific experiment. Vague or ambiguous jargon can lead to confusion and may relegate valuable signals to wasteful noise. For this reason, measured values must be expressed in standardized units for each parameter used to define mitochondrial respiratory function. Standardization of nomenclature and technical terms is essential to improve the awareness of the intricate meaning of divergent scientific vocabulary. The focus on coupling states in mitochondrial preparations is a first step

in the attempt to generate a harmonized and conceptually oriented nomenclature in bioenergetics and mitochondrial physiology. Coupling states of intact cells and respiratory control by fuel substrates and specific inhibitors of respiratory enzymes will be reviewed in subsequent communications.

2. Respiratory coupling states in mitochondrial preparations

> '*Every professional group develops its own technical jargon for talking about matters of critical concern ... People who know a word can share that idea with other members of their group, and a shared vocabulary is part of the glue that holds people together and allows them to create a shared culture*' (Miller 1991).

2.1. Definitions

Mitochondrial preparations are defined as either isolated mitochondria, or tissue and cellular preparations in which the barrier function of the plasma membrane is disrupted. The plasma membrane separates the cytosol, nucleus and organelles (the intracellular compartment) from the environment of the cell. The plasma membrane consists of a lipid bilayer, embedded proteins and attached organic molecules which collectively control the selective permeability of ions, organic molecules and particles across the cell boundary. The intact plasma membrane, therefore, prevents the passage of many water-soluble mitochondrial substrates, such as succinate or ADP, that are required for the analysis of respiratory capacity at kinetically saturating concentrations, thus limiting the scope of investigations into mitochondrial respiratory function in intact cells. The cholesterol content of the plasma membrane is high compared to mitochondrial membranes. Therefore, mild detergents, such as digitonin and saponin, can be applied to selectively permeabilize the plasma membrane by interaction with cholesterol and allow free exchange of cytosolic components with ions and organic molecules of the immediate cell environment, while maintaining the integrity and localization of

organelles, cytoskeleton and the nucleus. Application of optimum concentrations of these mild detergents leads to the complete loss of cell viability, tested by nuclear staining, while mitochondrial function remains unaffected, as shown by the lack of a respiratory response of respiration of isolated mitochondria to the addition of such low concentrations of digitonin and saponin. Mechanical or chemical permeabilization is applied in tissue homogenates containing all components of the cell in the crude homogenate at highly diluted concentrations. Likewise, in permeabilized tissues or cells the functional and structural integrity of mitochondria are largely maintained. All mitochondria are retained in chemically permeabilized mitochondrial preparations and crude tissue homogenates. In the preparation of isolated mitochondria the cells or tissues are homogenized, and the mitochondria are separated from other cell fractions and purified by centrifugation, entailing the loss of a significant fraction of mitochondria. The term mitochondrial preparation does not include further fractionation of mitochondrial components, as well as submitochondrial particles.

Control and regulation: The terms metabolic *control* and *regulation* are frequently used synonymously, but are distinguished in metabolic control analysis: 'We could understand the regulation as the mechanism that occurs when a system maintains some variable constant over time, in spite of fluctuations in external conditions (homeostasis of the internal state). On the other hand, metabolic control is the power to change the state of the metabolism in response to an external signal' (Fell 1997). Respiratory control may be induced by experimental control signals that *exert* an influence on: (*1*) ATP demand and ADP phosphorylation rate; (*2*) fuel substrate, pathway competition and oxygen availability, *e.g.*, starvation and hypoxia; (*3*) the protonmotive force, redox states, flux-force relationships, coupling and efficiency; (*4*) Ca^{2+} and other ions including H^{+}; (*5*) inhibitors, *e.g.*, nitric oxide or intermediary metabolites, such as oxaloacetate. *Mechanisms* of respiratory control and regulation include adjustments of (*1*) enzyme activities by allosteric mechanisms and phosphorylation, (*2*) enzyme content, concentrations of cofactors and conserved moieties (such as adenylates, nicotinamide adenine

dinucleotide [NAD^+/NADH], coenzyme Q, cytochrome *c*); (*3*) metabolic channeling by supercomplexes; and *(4)* mitochondrial density (enzyme concentrations and membrane area) and morphology (cristae folding, fission and fusion). (*5*) Mitochondria are targeted directly by hormones, thereby affecting their energy metabolism (Lee *et al.* 2013; Gerö and Szabo 2016; Price and Dai 2016; Moreno *et al.* 2017). Evolutionary or acquired differences in the genetic and epigenetic basis of mitochondrial function (or dysfunction) between subjects and gene therapy; age; gender, biological sex, and hormone concentrations; life style including exercise and nutrition; and environmental issues including thermal, atmospheric, toxicological and pharmacological factors, exert an influence on all control mechanisms listed above (for reviews, see Brown 1992; Gnaiger 1993a, 2009; 2014; Paradies *et al.* 2014; Morrow *et al*. 2017).

Respiratory control and response: There is a difference between control by a fixed component of a metabolic system or module, e.g. ATP synthase, and the response to an experimental variable, *e.g.*, fuel substrate or ADP. Whilst lack of control by a metabolic module, *e.g.* phosphorylation system, does mean that there will be no response to a variable activating it, *e.g.* [ADP], the reverse is not true; *i.e.*, lack of response to [ADP] does not exclude the phosphorylation system from having some degree of control. The degree of control of a component of the OXPHOS system on an output variable of the system, such as oxygen flux, will in general be different from the degree of control on other outputs, such as phosphorylation flux, cytochrome redox states, protonmotive force, phosphorylation potential, and proton leak flux (**Table 1**). As such, it is necessary to be specific as to which output is under consideration. Respiratory control is insufficiently specific in the context of specific interpretations (Fell 1997).

Respiratory coupling control: Respiratory control is monitored in a mitochondrial preparation under conditions defined as respiratory states. When phosphorylation of ADP to ATP is stimulated or depressed, an increase or decrease is observed in electron flow linked to oxygen consumption in ‘controlled’ coupling states in intact mitochondria. Alternatively,

coupling of electron transfer with phosphorylation is disengaged by disruption of the integrity of the inner mitochondrial membrane or by uncouplers, functioning like a clutch in a mechanical system. The corresponding coupling control state is characterized by high levels of oxygen consumption without control by phosphorylation ('uncontrolled state'; classical terminology). Energetic coupling is defined in **Box 2**. Respiratory control refers to the ability of mitochondria to adjust oxygen consumption in response to external control signals by engaging various mechanisms of control and regulation. Loss of coupling by intrinsic uncoupling and decoupling, or pathological dyscoupling lowers the efficiency. Such generalized uncoupling is different from switching to mitochondrial pathways that involve fewer than three proton pumps ('coupling sites': Complexes CI, CIII and CIV), bypassing CI through multiple electron entries into the Q-junction (**Fig. 1**). A bypass of CIII and CIV is provided by alternative oxidases, which reduce oxygen without proton translocation. Reprogramming of mitochondrial pathways may be considered as a switch of gears (changing the stoichiometry) rather than uncoupling (loosening the stoichiometry).

Pathway control states are obtained in mitochondrial preparations by depletion of endogenous substrates and addition to the mitochondrial respiration medium of fuel substrates (CHNO) and specific inhibitors, activating selected mitochondrial pathways (**Fig. 1**). Coupling control states and pathway control states are complementary, since mitochondrial preparations depend on an exogenous supply of pathway-specific fuel substrates and oxygen (Gnaiger 2014).

2.2. Three coupling states of mitochondrial preparations and residual oxygen consumption

Coupling control states: To extend the classical nomenclature on mitochondrial coupling states (Section 2.3) by a concept-driven terminology that incorporates explicit information on the nature of the respiratory states, the terminology must be general and not restricted to any particular experimental protocol or mitochondrial preparation (Gnaiger 2009). We focus primarily on the conceptual 'why', along with clarification of the experimental 'how'.

In the following section, the concept-driven terminology is explained and coupling states are defined. The capacity of *oxidative phosphorylation*, OXPHOS, provides diagnostic reference values for physiological respiratory capacities of defined pathways of core energy metabolism and is, therefore, measured at kinetically saturating concentrations of ADP and inorganic phosphate, P_i. The *oxidative* capacity of the electron transfer system, ETS, reveals the limitation of OXPHOS capacity mediated by the *phosphorylation* system. ETS capacity is measured as noncoupled respiration by application of *external uncouplers*. The contribution of *intrinsically uncoupled* oxygen consumption is most easily studied by not stimulating or arresting phosphorylation, when oxygen consumption compensates mainly for the proton leak; the corresponding states are collectively classified as LEAK states (**Table 1**). Coupling states of mitochondrial preparations can be compared in any defined mitochondrial pathway control state (**Fig. 1**). Fuel substrates and ETS inhibitors are kept constant while (*1*) adding ADP or P_i, (*2*) inhibiting the phosphorylation system, and (*3*) performing uncoupler titrations.

Respiratory capacities and kinetic control: Coupling control states are established in the study of mitochondrial preparations to obtain reference values for various output variables. Physiological conditions *in vivo* may deviate substantially from these experimentally obtained states. Since kinetically saturating concentrations, *e.g.* of ADP or oxygen, may not apply to physiological intracellular conditions, relevant information is obtained in studies of kinetic responses to conditions intermediate between the LEAK state at zero [ADP] and the OXPHOS state at saturating [ADP], or of respiratory capacities in the range between kinetically saturating [O_2] and anoxia (Gnaiger 2001). We define respiratory capacities, comparable to channel capacity in information theory, as the upper bound of the rate of respiration measured in defined coupling and pathway control states of mitochondrial preparations.

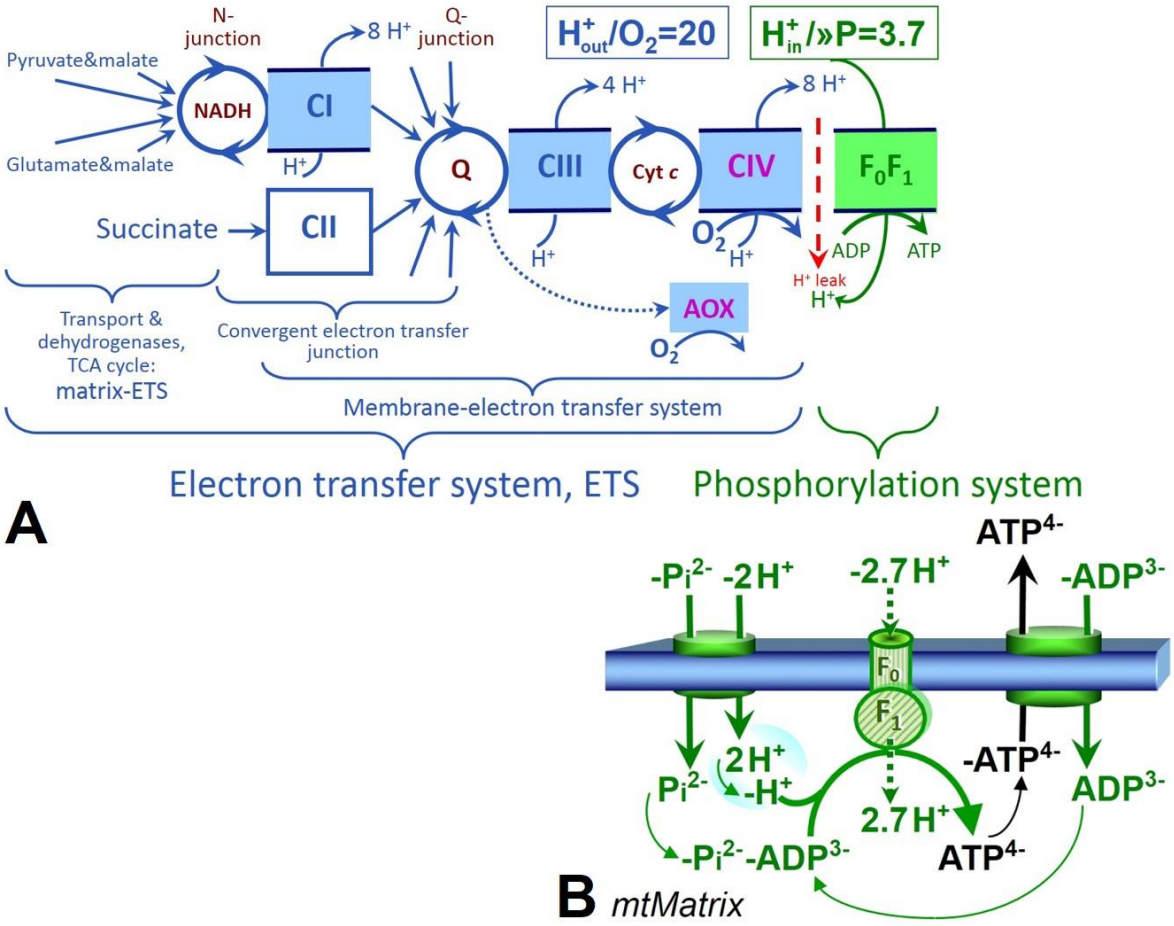

Fig. 1. The mitochondrial respiratory system and oxidative phosphorylation. (A) The electron transfer system, ETS, and coupling to the phosphorylation system. Multiple convergent electron transfer pathways are shown from NADH and succinate; additional arrows indicate electron entry through electron transferring flavoprotein, glycerophosphate dehydrogenase, dihydro-orotate dehydrogenase, choline dehydrogenase, and sulfide-ubiquinone oxidoreductase. The branched pathway of oxygen consumption by alternative quinol oxidase (AOX) is indicated by the dotted arrow. H^+_{out}/O_2 is the ratio of outward proton flux from the matrix space to catabolic O_2 flux in the NADH-linked pathway. $H^+_{in}/»P$ is the ratio of inward proton flux from the inter-membrane space to the endergonic flux of phosphorylation of ADP to ATP. Due to proton leak and slip these are not fixed stoichiometries. (**B**) Phosphorylation system consisting of the F_1F_0 ATP synthase, adenine nucleotide translocase, and the inorganic phosphate transporter. The $H^+_{in}/»P$ stoichiometry is the sum of the coupling stoichiometry in the ATP synthase reaction (-2.7 H^+ from the intermembrane space, 2.7 H^+ to the matrix) and the proton balance in the translocation of ADP^{2-}, ATP^{3-} and P_i^{2-}. See Eqs. 11 and 12 for further explanation. Modified from (A) Lemieux *et al*. (2017) and (B) Gnaiger (2014).

Phosphorylation, »P: *Phosphorylation* in the context of OXPHOS is defined as phosphorylation of ADP to ATP. On the other hand, the term phosphorylation is used generally in many different contexts, *e.g.* protein phosphorylation. This justifies consideration of a symbol more discriminating and specific than P as used in the P/O ratio (phosphate to atomic oxygen ratio), where P indicates phosphorylation of ADP to ATP or GDP to GTP. We propose the symbol »P for the endergonic direction of phosphorylation ADP→ATP, and likewise the symbol «P for the corresponding exergonic hydrolysis ATP→ADP (**Fig. 2**). ##ATP synthase is the proton pump of the phosphorylation system (**Fig. 1B**). »P may also involve substrate-level phosphorylation as part of the tricarboxylic acid cycle (succinyl-CoA ligase) and phosphorylation of ADP catalyzed by phosphoenolpyruvate carboxykinase, adenylate kinase, creatine kinase, hexokinase and nucleoside diphosphate kinase (NDPK). Kinase cycles are involved in intracellular energy transfer and signal transduction for regulation of energy flux. In isolated mammalian mitochondria ATP production catalyzed by adenylate kinase, 2ADP ↔ ATP + AMP, proceeds without fuel substrates in the presence of ADP (Komlódi and Tretter 2017). $J_{»P}/J_{O2}$ (»P/O_2) is two times the 'P/O' ratio of classical bioenergetics. The effective »P/O_2 ratio is diminished by: (*1*) the proton leak across the inner mitochondrial membrane from low pH in the P-phase to high pH in the N-phase (P, positive; N, negative); (*2*) cycling of other cations; (*3*) proton slip in the proton pumps when a proton effectively is not pumped; and (*4*) electron leak in the univalent reduction of oxygen (O_2; dioxygen) to superoxide anion radical ($O_2^{\bullet-}$).

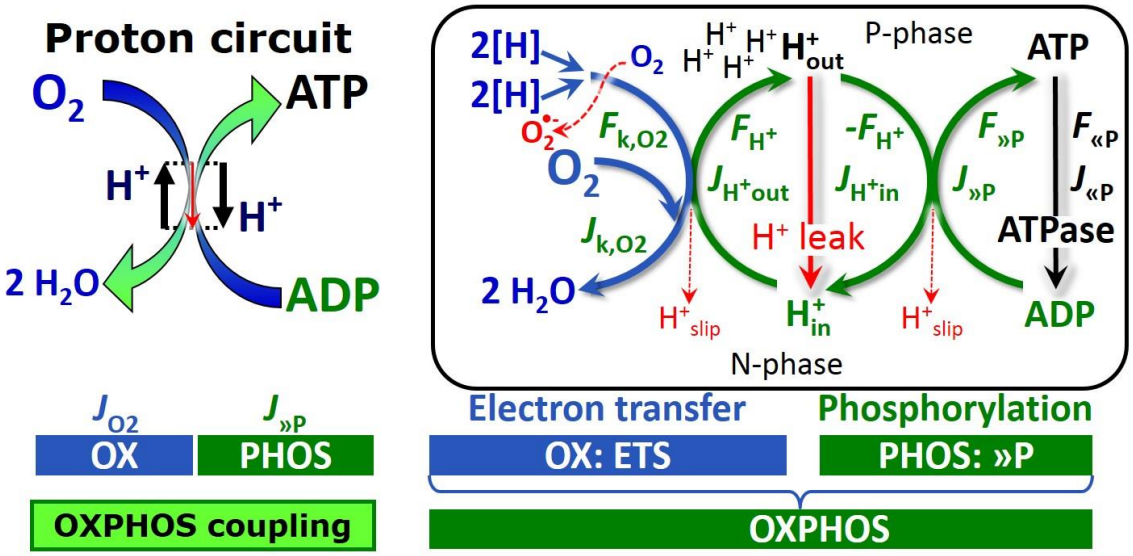

Fig. 2. The proton circuit and coupling in oxidative phosphorylation (OXPHOS). Oxygen flux, $J_{k,O2}$, in a catabolic reaction k is coupled to the phosphorylation of ADP to ATP, $J_{»P}$, by the proton pumps of the electron transfer system, ETS, pushing the outward proton flux, J_{H+out}, and generating the output protonmotive force, $F_{H+} \equiv F_{H+out}$. ATP synthase is coupled to inward proton flux, J_{H+in}, to phosphorylate ADP to ATP, driven by the input protonmotive force, $F_{H+in} = -F_{H+}$. 2[H] indicates the reduced hydrogen equivalents of fuel substrates that provide the chemical input force, $F_{k,O2}$ [kJ/mol O_2], of the catabolic reaction k with oxygen (Gibbs energy of reaction per mole O_2 consumed in reaction k), typically in the range of -460 to -480 kJ/mol. The output force is given by the phosphorylation potential difference (ADP phosphorylated to ATP), $F_{»P}$, which varies *in vivo* ranging from about 48 to 62 kJ/mol under physiological conditions. Fluxes, J_B, and forces, F_B, are expressed in either chemical units, [mol·s^{-1}·L^{-1}] and [J·mol^{-1}] respectively, or electrical units, [C·s^{-1}·L^{-1}] and [J·C^{-1}] respectively, per volume, V [L], of the system (defined by the system boundaries shown as the black line). Modified from Gnaiger (2014).

Box 2: Coupling, power and efficiency, at constant temperature and pressure

Energetic coupling means that two processes of energy transformation are linked such that the input power, P_{in}, is the driving element of the output power, P_{out}, and the out/input power ratio is the efficiency. In general, power is work per unit time [J.s^{-1}=W]. When describing a system with volume V without information on the internal structure, the output is defined as the *external* work (exergy) performed by the *total* system on its environment. Such as system may be open

for any type of exchange, or closed and thus allowing only heat and work to be exchanged across the system boundaries. This is the classical black box approach of thermodynamics. In contrast, in a colourful compartmental analysis of *internal* energy transformations (**Fig. 2**), the system is structured and described by definition of internal compartments (with information on the heterogeneity of the system) and analysis of separate parts, *i.e.* a sequence of *partial* energy transformations, tr. In general, power per unit volume, P_{tr}/V [W.L^{-1}], is the product of a volume-specific flux, J_{tr}, and its conjugated force, F_{tr}, and is closely linked to the dissipation function using the terminology of irreversible thermodynamics (Prigogine 1967; Gnaiger 1993a,b). In **Fig. 2**, the scalar catabolic reaction of oxygen consumption is expressed as oxygen flux per volume, $J_{k,O2}$. It is coupled to vectorial translocation of protons across the inner mitochondrial membrane, from the negative compartment (matrix) to the positive compartment (inter-membrane space). Compartmental vectorial translocation does not, however, implicate a vector force or gradient across the membrane with defined spatial direction, but the protonmotive force is defined merely as an electrochemical potential difference between two compartments. Output power of proton translocation and catabolic input power are (**Fig. 2**),

Output: $$P_{H+out}/V = J_{H+out} \cdot F_{H+}$$

Input: $$P_k/V = J_{k,O2} \cdot F_{k,O2}$$

$F_{k,O2}$ is the exergonic input force with a negative sign, and, F_{H+}, is the endergonic output force with a positive sign (**Box 3**). Ergodynamic efficiency is the ratio of output/input power, or the flux ratio times force ratio (Gnaiger 1993a,b),

$$\varepsilon = \frac{P_{H+out}}{-P_k} = \frac{J_{H+out}}{J_{k,O2}} \cdot \frac{F_{H+}}{-F_{k,O2}}$$

The concept of incomplete coupling relates exclusively to the first term, *i.e.* the flux ratio, or H^+_{out}/O_2 ratio (**Fig. 1**). Likewise, respirometric definitions of the »P/O_2 ratio and biochemical coupling efficiency (Section 3.2) consider flux ratios. In a completely coupled process, the power efficiency, ε, depends entirely on the force ratio, ranging from zero efficiency at an

output force of zero, to the limiting output force and maximum efficiency of 1.0, when the total power of the coupled process, $P_t=P_k+P_{H+out}$, equals zero, and any net flows are zero at ergodynamic equilibrium of a coupled process. Thermodynamic equilibrium is defined as the state when all potentials (all forces) are dissipated and equilibrate towards their minima of zero. In a fully or completely coupled process, output and input fluxes are directly proportional in a fixed ratio technically defined as a stoichiometric relationship (a gear ratio in a mechanical system). Such maximal stoichiometric output/input flux ratios are considered in OXPHOS analysis as the upper limits or mechanistic H^+_{out}/O_2 and »P/O_2 ratios (**Fig. 1**).

The steady-state: Mitochondria represent a thermodynamically open system functioning as a biochemical transformation system in non-equilibrium states. State variables (protonmotive force; redox states) and metabolic fluxes (*rates*) are measured in defined mitochondrial respiratory *states*. Strictly, steady states can be obtained only in open systems, in which changes due to *internal* transformations, *e.g.*, O_2 consumption, are instantaneously compensated for by *external* flows *e.g.*, O_2 supply, such that oxygen concentration does not change in the system (Gnaiger 1993b). Mitochondrial respiratory states monitored in closed systems satisfy the criteria of pseudo-steady states for limited periods of time, when changes in the system (concentrations of O_2, fuel substrates, ADP, P_i, H^+) do not exert significant effects on metabolic fluxes (respiration, phosphorylation). Such pseudo-steady states require respiratory media with sufficient buffering capacity and kinetically saturating concentrations of substrates to be maintained, and thus depend on the kinetics of the processes under investigation. Proton turnover, $J_{\infty H+}$, and ATP turnover, $J_{\infty P}$, proceed in the steady-state at constant F_{H+}, when $J_{\infty H+} = J_{H+out} = J_{H+in}$, and at constant $F_{»P}$, when $J_{\infty P} = J_{»P} = J_{«P}$ (**Fig. 2**).

Table 1. Coupling states and residual oxygen consumption in mitochondrial preparations in relation to respiration and phosphorylation rate, J_{O2} and $J_{»P}$, and protonmotive force, F_{H+}. Coupling states are established at kinetically saturating concentrations of fuel substrates and O_2.

State	J_{O2}	$J_{»P}$	F_{H+}	Inducing factors	Limiting factors
LEAK	*L*; low proton leak-dependent respiration;	0	max.	Proton leak, slip, and cation cycling	$J_{»P}$=0: (*1*) without ADP, L_N; (*2*) max. ATP/ADP ratio, L_T; or (*3*) inhibition of the ADP phosphorylation system, L_{Omy}
OXPHOS	*P*; high ADP-stimulated respiration	max.	high	Kinetically saturating [ADP] and [P_i]	$J_{»P}$ by phosphorylation system; or J_{O2} by electron transfer system
ETS	*E*; max. noncoupled respiration	0	low	Optimal external uncoupler concentration for maximum oxygen flux	J_{O2} by electron transfer system
ROX	*Rox*; min. residual O_2 consumption	0	0	Non-ETS oxidation reactions	Full inhibition of ETS or absence of substrates

LEAK state (Fig. 3): LEAK state is defined as a state of mitochondrial respiration when O_2 flux mainly compensates for the proton leak in the absence of ATP synthesis, at kinetically saturating concentrations of O_2 and respiratory substrates. LEAK respiration is measured to obtain an indirect estimate of *intrinsic*

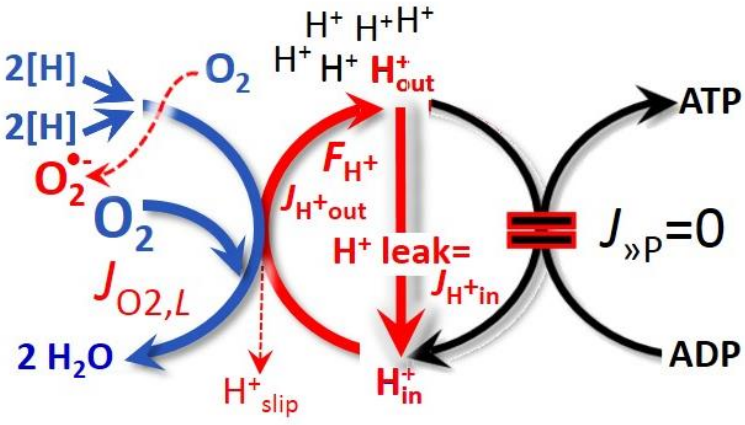

Fig. 3. LEAK state: Phosphorylation is arrested, $J_{»P}$=0, and oxygen flux, $J_{O2,L}$, is controlled mainly by the proton leak, which equals $J_{H^+in,}$ at maximum protonmotive force, F_{H+} (See also Fig. 2).

uncoupling without addition of any experimental uncoupler: (*1*) in the absence of adenylates; (*2*) after depletion of ADP at maximum ATP/ADP ratio; or (*3*) after inhibition of the phosphorylation system by inhibitors of ATP synthase, such as oligomycin, or adenine nucleotide translocase, such as carboxyatractyloside.

Proton leak: Proton leak is the *uncoupled* process in which protons are translocated across the inner mitochondrial membrane in the dissipative direction of the downhill protonmotive force without coupling to phosphorylation (**Fig. 3**). The proton leak flux depends on the protonmotive force, is a property of the inner mitochondrial membrane, may be enhanced due to possible contaminations by free fatty acids, and is physiologically controlled. In particular, uncoupling mediated by uncoupling protein 1 (UCP1) is physiologically controlled, *e.g.*, in brown adipose tissue. UCP1 is a proton channel of the inner mitochondrial membrane facilitating the conductance of protons across the inner mitochondrial membrane. As consequence of this effective short-circuit, the protonmotive force diminishes, resulting in stimulation of electron transfer to oxygen and heat dissipation without phosphorylation of ADP. Mitochondrial injuries may lead to *dyscoupling* as a pathological or toxicological cause of *uncoupled* respiration, *e.g.*, as a consequence of opening the permeability transition pore. Dyscoupled respiration is distinguished from the experimentally induced *noncoupled* respiration in the ETS state. Under physiological conditions, the proton leak is the dominant contributor to the overall leak current.

Proton slip: Proton slip is the *decoupled* process in which protons are only partially translocated by a proton pump of the ETS and slip back to the original compartment (Dufour *et al.* 1996). Proton slip can also happen in association with the ATP-synthase, in which case the proton slips downhill across the membrane to the matrix without contributing to ATP synthesis. In each case, proton slip is a property of the proton pump and increases with the turnover rate of the pump.

Cation cycling: Proton leak is a leak current of protons. There can be other cation contributors to leak current including calcium and probably magnesium. Calcium current is balanced by mitochondrial Na/Ca exchange, which is balanced by Na/H exchange or K/H exchange. This is another effective uncoupling mechanism different from proton leak and slip.

Small differences of terms, *e.g.*, uncoupled, noncoupled, are easily overlooked and may be erroneously perceived as identical. Even with an attempt at rigorous definition, the common use of such terms may remain vague (**Table 2**).

OXPHOS state (**Fig. 4**): OXPHOS state is defined as the respiratory state with kinetically saturating concentrations of O_2, respiratory and phosphorylation substrates, and absence of exogenous uncoupler, which provides an estimate of the maximal capacity of OXPHOS in any given pathway control state.

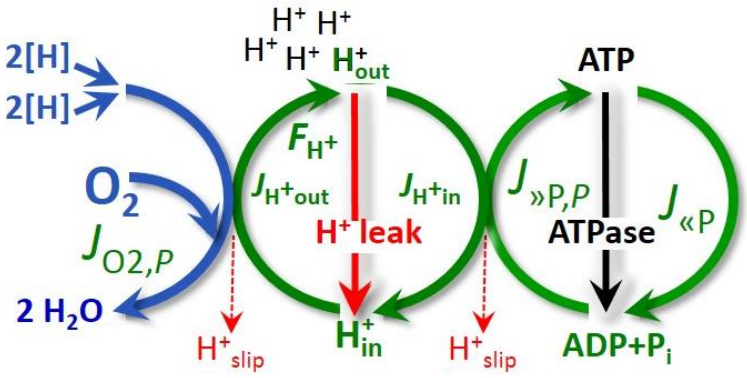

Fig. 4. OXPHOS state: Phosphorylation, $J_{»P}$, is stimulated by kinetically saturating [ADP] and inorganic phosphate, [P_i], and is supported by a high protonmotive force, F_{H+}. O_2 flux, $J_{O2,P}$, is highly coupled at a maximum »P/O_2 ratio, $J_{»P,P}/J_{O2,P}$ (See also Fig. 2).

Respiratory capacities at kinetically saturating substrate concentrations provide reference values or upper limits of performance, aiming at the generation of data sets for comparative purposes. Any effects of substrate kinetics are thus separated from reporting actual mitochondrial capacity for oxidation during coupled respiration, against which physiological activities can be evaluated.

As discussed previously, 0.2 mM ADP does not fully saturate flux in isolated mitochondria (Gnaiger 2001; Puchowicz *et al.* 2004); greater ADP concentration is required, particularly in permeabilized muscle fibres and cardiomyocytes, to overcome limitations by intracellular diffusion and by the reduced conductance of the outer mitochondrial membrane

(Jepihhina *et al.* 2011, Illaste *et al.* 2012, Simson *et al*. 2016) either through interaction with tubulin (Rostovtseva *et al.* 2008) or other intracellular structures (Birkedal *et al*. 2014). In permeabilized muscle fibre bundles of high respiratory capacity, the apparent K_m for ADP increases up to 0.5 mM (Saks *et al.* 1998), indicating that >90% saturation is reached only at >5 mM ADP. Similar ADP concentrations are also required for accurate determination of OXPHOS capacity in human clinical cancer samples and permeabilized cells (ref).

Table 2. Distinction of terms related to coupling.

Term	Respiration	»P/O₂	Note
Fully coupled	*P* – *L*	Max.	OXPHOS capacity corrected for LEAK respiration (**Fig. 6**)
Coupled	*P*	High	Phosphorylating respiration with a variable component of intrinsic LEAK respiration (**Fig. 4**)
Uncoupled, Decoupled	*L*	0	Non-phosphorylating respiration without added protonophore (**Fig. 3**)
Noncoupled	*E*	0	Non-phosphorylating respiration stimulated to maximum flux at optimum uncoupler concentration (**Fig. 5**)
Dyscoupled	*P*	Low	Pathologically increased uncoupling, mitochondrial dysfunction

ETS state (**Fig. 5**): The ETS state is defined as the *noncoupled* state with kinetically saturating concentrations of O_2, respiratory substrate and optimum *exogenous* uncoupler concentration for maximum O_2 flux, as an estimate of oxidative ETS capacity. Inhibition of respiration is observed at higher than optimum uncoupler concentrations. As a consequence of

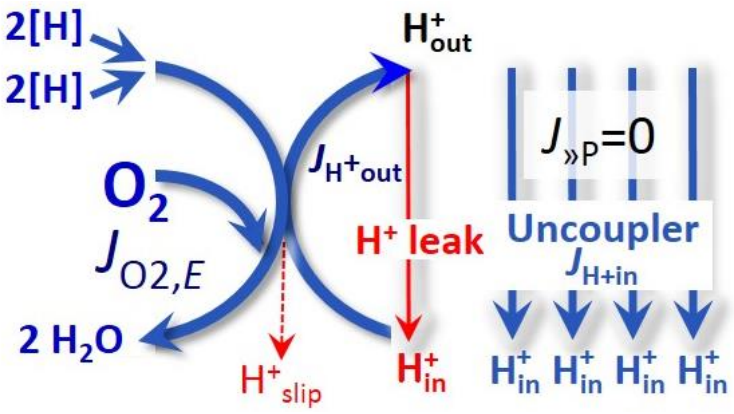

Fig. 5. ETS state: Noncoupled respiration, $J_{O2,E}$, is maximum at optimum exogenous uncoupler concentration and phosphorylation is zero, $J_{»P}=0$ (See also Fig. 2).

the nearly collapsed protonmotive force, the driving force is insufficient for phosphorylation and $J_{»P}$=0.

Besides the three fundamental coupling states of mitochondrial preparations, the following respiratory state also is relevant to assess respiratory function:

ROX: Residual oxygen consumption (ROX) is defined as O_2 consumption due to oxidative side reactions remaining after inhibition of the ETS. ROX is not a coupling state but represents a baseline that is used to correct mitochondrial respiration in defined coupling states. ROX is not necessarily equivalent to non-mitochondrial respiration, considering oxygen-consuming reactions in mitochondria not related to ETS, such as oxygen consumption in reactions catalyzed by monoamine oxidases (type A and B), monooxygenases (cytochrome P450 monooxygenases), dioxygenase (sulfur dioxygenase and trimethyllysine dioxygenase), several hydoxylases, and more. Mitochondrial preparations, especially those obtained from liver, are contaminated by peroxisomes. This fact makes the exact determination of mitochondrial oxygen consumption and mitochondria-associated generation of reactive oxygen species complicated (Schönfeld *et al.* 2009). The dependence of ROX-linked oxygen consumption needs to be studied in detail with respect to non-ETS enzyme activities, availability of specific substrates, oxygen concentration, and electron leakage leading to the formation of reactive oxygen species.

2.3. Classical terminology for isolated mitochondria

> *'When a code is familiar enough, it ceases appearing like a code; one forgets that there is a decoding mechanism. The message is identical with its meaning'* (Hofstadter 1979).

Chance and Williams (1955; 1956) introduced five classical states of mitochondrial respiration and cytochrome redox states. **Table 3** shows a protocol with isolated mitochondria in a closed respirometric chamber, defining a sequence of respiratory states.

Table 3. Metabolic states of mitochondria (Chance and Williams, 1956; Table V).

State	$[O_2]$	ADP level	Substrate level	Respiration rate	Rate-limiting substance
1	>0	low	low	slow	ADP
2	>0	high	~0	slow	Substrate
3	>0	high	high	fast	respiratory chain
4	>0	low	high	slow	ADP
5	0	high	high	0	Oxygen

State 1 is obtained after addition of isolated mitochondria to air-saturated isoosmotic/isotonic respiration medium containing inorganic phosphate, but no fuel substrates and no adenylates, *i.e.*, AMP, ADP, ATP.

State 2 is induced by addition of a high concentration of ADP (typically 100 to 300 µM), which stimulates respiration transiently on the basis of endogenous fuel substrates and phosphorylates only a small portion of the added ADP. State 2 is then obtained at a low respiratory activity limited by zero endogenous fuel substrate availability (**Table 3**). If addition of specific inhibitors of respiratory complexes, such as rotenone, does not cause a further decline of oxygen consumption, State 2 is equivalent to residual oxygen consumption (See below). If inhibition is observed, undefined endogenous fuel substrates are a confounding factor of pathway control by externally added substrates and inhibitors. In contrast to the original definition, an alternative protocol is frequently applied, in which State 2 is induced by addition of fuel substrate without ADP (LEAK state), followed by addition of ADP.

State 3 is the state stimulated by addition of fuel substrates while the ADP concentration is still high (**Table 3**) and supports coupled energy transformation through oxidative phosphorylation. 'High ADP' is a concentration of ADP specifically selected to allow the measurement of State 3 to State 4 transitions of isolated mitochondria in a closed respirometric system. Repeated ADP titration re-establishes State 3 at ‘high ADP’. Starting at oxygen concentrations near air-saturation (ca. 200 µM O_2 at sea level and 37 °C), the total ADP

608 concentration added must be low enough (typically 100 to 300 µM) to allow phosphorylation
609 to ATP at a coupled oxygen consumption that does not lead to oxygen depletion during the
610 transition to State 4. In contrast, kinetically saturating ADP concentrations usually are an order
611 of magnitude higher than 'high ADP', *e.g.* 2.5 mM in isolated mitochondria. The abbreviation
612 State 3u is frequently used in bioenergetics, to indicate the state of respiration after titration of
613 an uncoupler, without sufficient emphasis on the fundamental difference between OXPHOS
614 capacity (*well-coupled* with an *endogenous* uncoupled component) and ETS capacity
615 (*noncoupled*).

616 **State 4** is a LEAK state which is obtained only if the mitochondrial preparation is intact
617 and well-coupled. Depletion of ADP by phosphorylation to ATP leads to a decline in oxygen
618 consumption in the transition from State 3 to State 4. Under these conditions, a maximum
619 protonmotive force and high ATP/ADP ratio are maintained, and the »P/O_2 ratio can be
620 calculated. State 4 respiration, L_T (**Table 1**), reflects intrinsic proton leak and intrinsic ATP
621 hydrolysis activity. Oxygen consumption in State 4 is an overestimation of LEAK respiration
622 if the contaminating ATP hydrolysis activity recycles some ATP to ADP, $J_{«P}$, which stimulates
623 respiration coupled to phosphorylation, $J_{»P}>0$. This can be tested by inhibition of the
624 phosphorylation system using oligomycin, ensuring that $J_{»P}=0$ (State 4o). Alternatively,
625 sequential ADP titrations re-establish State 3, followed by State 3 to State 4 transitions while
626 sufficient oxygen is available. However, anoxia may be reached before exhaustion of ADP
627 (State 5).

628 **State 5** is the state after exhaustion of oxygen in a closed respirometric chamber.
629 Diffusion of oxygen from the surroundings into the aqueous solution may be a confounding
630 factor preventing complete anoxia (Gnaiger 2001).

631 In **Table 3**, only States 3 and 4 (and 'State 2' in the alternative protocol without ADP;
632 not included in the table) are coupling control states, with the restriction that O_2 flux in State 3
633 may be limited kinetically by non-saturating ADP concentrations (**Table 1**).

634

635 *2.4. Coupling states and respiratory rates*

636 It is important to distinguish metabolic systems or modules from metabolic states and the
637 corresponding metabolic rates; for example: electron transfer system, ETS (**Fig. 6**), ETS state
638 (**Fig. 5**), and ETS capacity, *E*, respectively (**Table 1**). The protonmotive force is *high* in the
639 OXPHOS state when it drives phosphorylation, *maximum* in the LEAK state of coupled
640 mitochondria, driven by LEAK respiration at a minimum back flux of protons to the matrix
641 side, and *very low* in the ETS state when uncouplers short-circuit the proton cycle (**Table 1**).

642

643 **Fig. 6. Four-compartment model of oxidative phosphorylation.** Respiratory states (ETS, OXPHOS,
644 LEAK) and corresponding rates (*E*, *P*, *L*) are connected by the protonmotive force, F_{H+}. Electron
645 transfer system capacity, *E*, is partitioned into the dissipative LEAK respiration, *L*, partial conservation of the protonmotive exergy (**Box 3**) as the phosphorylation exergy in net OXPHOS capacity, *P-L*, and the excess capacity, *E-P*. Modified from Gnaiger (2014).

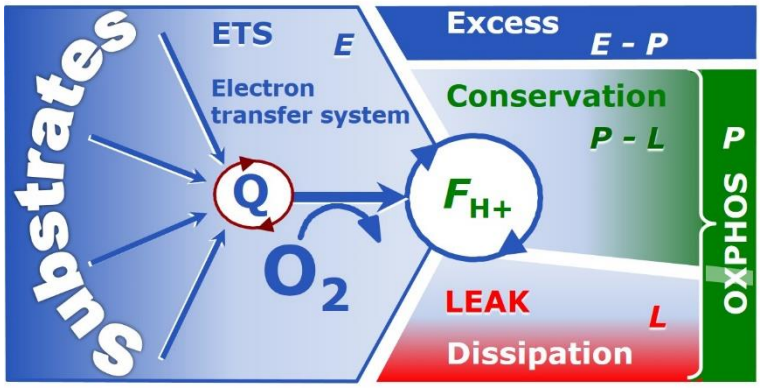

653

654 The three coupling states, ETS, LEAK and OXPHOS, are presented in a schematic
655 context with the corresponding respiratory rates, abbreviated as *E*, *L* and *P*, respectively (**Fig.**
656 **6**). This clarifies that *E* may exceed or be equal to *P*, but *E* cannot theoretically be lower than
657 *P*. *E*<*P* must be discounted as an artefact, which may be caused experimentally by: (*1*) loss of
658 oxidative capacity during the time course of the respirometric assay, since *E* is measured
659 subsequently to *P*; (*2*) using too low uncoupler concentrations; (*3*) using high uncoupler
660 concentrations which inhibit the ETS (Gnaiger 2008); (*4*) high oligomycin concentrations
661 applied for measurement of *L* before titrations of uncoupler, when oligomycin exerts an

662 inhibitory effect on *E*. On the other hand, the excess ETS capacity is overestimated if non-
663 saturating [P_i] or [ADP] (State 3) are used.

664 *E>P* is observed in many types of mitochondria, varying between species, tissues and cell
665 types. It is the excess ETS capacity pushing the phosphorylation system (**Fig. 1B**) to the limit
666 of its *capacity of utilizing* the protonmotive force. Within any type of mitochondria, the
667 magnitude of *E>P* depends on (*1*) the pathway control state with single or multiple electron
668 input into the Q-junction and involvement of three or fewer coupling sites determining the
669 H^+_{out}/O_2 *coupling stoichiometry* (**Fig. 1A**); and (*2*) the *biochemical coupling efficiency*
670 expressed as *(E-L)/E*, since an increase of *L* causes *P* to increase towards the limit of *E*. The
671 *excess E-P* capacity, *E-P*, therefore, provides a sensitive diagnostic indicator of specific injuries
672 of the phosphorylation system, under conditions when *E* remains constant but *P* declines
673 relative to controls (**Fig. 6**). Substrate cocktails supporting simultaneous convergent electron
674 transfer to the Q-junction for reconstitution of tricarboxylic acid cycle (TCA cycle) function
675 establish pathway control states with high ETS capacity, and consequently increase the
676 sensitivity of the *E-P* assay.

677 When subtracting *L* from *P*, the dissipative LEAK component in the OXPHOS state may
678 be overestimated. This can be avoided by measuring LEAK respiration in a state when the
679 protonmotive force is adjusted to its slightly lower value in the OXPHOS state, *e.g.*, by titration
680 of an ETS inhibitor. Any turnover-dependent components of proton leak and slip, however, are
681 underestimated under these conditions (Garlid *et al.* 1993). In general, it is inappropriate to use
682 the term *ATP production* for the difference of oxygen consumption measured in states *P* and *L*.
683 The difference *P-L* is the upper limit of the part of OXPHOS capacity that is freely available
684 for ATP production (corrected for LEAK respiration) and is fully coupled to phosphorylation
685 with a maximum mechanistic stoichiometry (**Fig. 6**).

686

687

3. States and rates

3.1. The protonmotive force and proton flow

The protonmotive force across the inner mitochondrial membrane (Mitchell and Moyle 1967) was introduced most beautifully in the *Grey Book 1966* (see Mitchell 2011),

$$\Delta p_{H+} = \Delta\Psi + \Delta\mu_{H+}/F \qquad \text{(Eq. 1)}$$

The protonmotive force consists of two partial forces: (*1*) The electrical part, $\Delta\Psi$, is the difference of charge (electric potential difference) and is not specific for H^+. (*2*) The chemical part, $\Delta\mu_{H+}$, is the chemical potential difference in H^+, is proportional to the pH difference, and incorporates the Faraday constant (**Table 4**).

Table 4. Protonmotive force and flow matrix. Rows: Electrical and chemical isomorphic format (*e* and *n*). The Faraday constant, *F*, converts protonmotive force and flow from *isomorphic format e* to *n*. Columns: The protonmotive force is the sum of *partial isomorphic forces* F_{el} and $F_{d,H+}$. In contrast to force (state), the conjugated flow (rate) cannot be partitioned.

State		**Force**		**electric**	**+**	**chemical**	**Unit**	**Notes**
	Protonmotive force, *e*	Δp_{H+}	=	$\Delta\Psi$	+	$\Delta\mu_{H+}/F$	$J\cdot C^{-1}$	Eq. 1*e*
	Chemiosmotic potential, *n*	$\Delta\tilde{\mu}_{H+}$	=	$\Delta\Psi\cdot F$	+	$\Delta\mu_{H+}$	$J\cdot mol^{-1}$	Eq. 1*n*
State	**Isomorph *e* and *n***	**Force,** $F_{H+/i}$	**=**	**el**	**+**	**d,H^+**		
	Electric charge, *e*	$F_{H+/e}$	=	$F_{el/e}$	+	$F_{d,H+/e}$	$J\cdot C^{-1}$	Eq. 2*e*
	Amount of substance, *n*	$F_{H+/n}$	=	$F_{el/n}$	+	$F_{d,H+/n}$	$J\cdot mol^{-1}$	Eq. 2*n*
Rate	**Isomorph *e* and *n***	**Flow,** $I_{H+/i}$	**=**	***e***	**or**	***N***		
	Electric charge, *e*	$I_{H+/e}$		$I_{H+/e}$			$C\cdot s^{-1}$	
	Amount of substance, *n*	$I_{H+/n}$				$I_{H+/n}$	$mol\cdot s^{-1}$	

Eq. 1: The Faraday constant, *F*, is the product of elementary charge (e=1.602177·10^{-19}·C) and the Avogadro (Loschmidt) constant (N_A=6.022136·10^{23}·mol^{-1}), $F=eN_A$=96,485.3 C/mol. $\Delta\tilde{\mu}_{H+}$ is the chemiosmotic potential difference. Eqs. 1*e* and 1*n* are the classical representations of Eqs. 2*e* and 2*n*.

Eq. 2: The protonmotive force is F_{H+}, expressed either in isomorphic format *e* or *n*. $F_{el/e} \equiv \Delta\Psi$ is the partial protonmotive force (el) acting generally on charged motive molecules (*i.e.* ions that are displaceable across the inner mitochondrial membrane). In contrast, $F_{d,H+/n} \equiv \Delta\mu_{H+}$ is the partial protonmotive force specific for proton displacement (d,H^+). The sign of the force is positive for endergonic, negative for exergonic transformations. The sign of the flow depends on the definition of the compartmental direction of the translocation (**Fig. 2**). Flow x force = $I_{H+/e} \cdot F_{H+/e}$ = $I_{H+/n} \cdot F_{H+/n}$ = Power [J/s=W].

Faraday constant, $F = eN_A$ [C/mol] (**Table 4**), enables the conversion between protonmotive force, $F_{H+/e} \equiv \Delta p_{H+}$ [J/C], expressed per *motive charge, e* [C], and protonmotive force or electrochemical potential difference, $F_{H+/n} \equiv \Delta\tilde{\mu}_{H+} = \Delta p_{H+} \cdot F$ [J/mol], expressed per *motive amount of protons, n* [mol]. Proton charge, *e*, and amount of substance, *n*, define the units for the isomorphic formats. Taken together, *F* converts protonmotive force and flow from isomorphic format *e* to *n* (Eq. 3; see also **Table 4**, Eq. 2),

$$F_{H+/n} = F_{H+/e} \cdot eN_A \qquad \text{(Eq. 3.1)}$$

$$I_{H+/n} = I_{H+/e} / (eN_A) \qquad \text{(Eq. 3.2)}$$

In each format, the protonmotive force is expressed as the sum of two partial forces. The concept expressed by the complex symbols in Eq. 1 can be explained and visualized more easily by *partial isomorphic forces* as the components of the protonmotive force:

Electrical part of the protonmotive force: (*1*) Isomorph *e:* $F_{el/e} \equiv \Delta\Psi$ is the electrical part of the protonmotive force expressed in units joule per coulomb, *i.e.* volt [V=J/C]. $F_{el/e}$ is defined as partial Gibbs energy change per *motive elementary charge, e* [C], not specific for proton charge (**Table 4**, Eq. 2*e*). (*2*) Isomorph *n:* $F_{el/n} \equiv \Delta\Psi \cdot F$ is the electric force expressed in units joule per mole [J/mol], defined as partial Gibbs energy change per *motive amount of charge, n* [mol], not specific for proton charge (**Table 4**, Eq. 2*n*).

Chemical part of the protonmotive force: (*1*) Isomorph *n:* $F_{d,H+/n} \equiv \Delta\mu_{H+}$ is the chemical part (diffusion, displacement of H^+) of the protonmotive force expressed in units joule per mole

736 [J/mol]. $F_{d,H+/n}$ is defined as partial Gibbs energy change per *motive amount of protons, n* [mol]
737 (**Table 4**, Eq. 2*n*). (*2*) Isomorph *e*: $F_{d,H+/e} \equiv \Delta\mu_{H+}/F$ is the chemical force expressed in units
738 joule per coulomb [V], defined as partial Gibbs energy change per *motive amount of protons*
739 *expressed in units of electric charge, e* [C], but specific for proton charge (**Table 4**, Eq. 2*e*).
740 Protonmotive means that there is a potential for the movement of protons, and force is a
741 measure of the potential for motion. Motion is relative and not absolute (Principle of Galilean
742 Relativity); likewise there is no absolute potential, but (isomorphic) forces are potential
743 differences (equations in **Table 5**). An electric partial force expressed in the format of electric
744 charge, $F_{el/e}$, of -0.2 V (Eq. 8*e*) is equivalent to force in the format of amount, $F_{el,H+/n}$, of 19
745 kJ·mol^{-1} H^+_{out} (Eq. 8*n*). For a ΔpH of 1 unit, the chemical partial force in the format of amount,
746 $F_{d,H+/n}$, changes by 5.9 kJ·mol^{-1} (Eq. 9*n*) and chemical force in the format of charge $F_{d,H+/e}$
747 changes by 0.06 V (**Table 5**, Eq. 9*e*). Considering a driving force of -470 kJ·mol^{-1} O_2 for
748 oxidation, the thermodynamic limit of the H^+_{out}/O_2 ratio is reached at a value of 470/19=24,
749 compared to a mechanistic stoichiometry of 20 (**Fig. 1**).
750
751 ---
752 **Box 3: Endergonic and exergonic transformations, exergy and dissipative loss**
753 A chemical reaction, or any transformation, is exergonic if the Gibbs energy change (exergy)
754 of the reaction is negative at constant temperature and pressure. The sum of Gibbs energy
755 changes of all internal transformations in a system can only be negative, i.e. exergy is
756 irreversibly dissipated. Endergonic reactions are characterized by positive Gibbs energies of
757 reaction and cannot proceed spontaneously in the forward direction as defined. For instance,
758 the endergonic reaction »P is coupled to exergonic catabolic reactions, such that the total Gibbs
759 energy change is negative, *i.e.* exergy must be dissipated for the reaction to proceed (**Fig. 2**).
760 In contrast, energy cannot be lost or produced in any internal process, which is the key
761 message of the first law of thermodynamics. Thus mitochondria are the sites of energy

762 transformation but not energy production. Open and closed systems can gain energy and exergy
763 only by external flows, *i.e.* uptake from the environment. Exergy is the potential to perform
764 work. In the framework of flux-force relationships (**Box 2**), the *partial* derivative of Gibbs
765 energy per advancement of a transformation is an isomorphic force, F_{tr} (**Table 5**, Eq. 5). In
766 other words, force is equal to exergy/motive unit (in integral form, this definition takes care of
767 non-isothermal processes). This formal generalization represents an appreciation of the
768 conceptual beauty of Peter Mitchell's innovation of the protonmotive force against the
769 background of the established paradigm of the electromotive force (emf) defined at the limit of
770 zero current (Cohen *et al.* 2008).

771 ---

772

773 **Table 5. Power, exergy, force, flow, and advancement.**
774

Expression	Symbol	Definition	Unit	Notes
Power	P_{tr}	$P_{tr} = I_{tr} \cdot F_{tr} = \partial_{tr}G \cdot \partial t^{-1}$	$W=J \cdot s^{-1}$	Eq. 4
Force, isomorphic	F_{tr}	$F_{tr} = \partial_{tr}G \cdot \partial_{tr}\xi^{-1}$	$J \cdot x^{-1}$	Eq. 5
Flow, isomorphic	I_{tr}	$I_{tr} = d_{tr}\xi \cdot dt^{-1}$	$x \cdot s^{-1}$	Eq. 6
Advancement, *n*	$d_{tr}\zeta_{H+/n}$	$d_{tr}\zeta_{H+/n} = dn_{H+} \cdot \nu_{H+}^{-1}$	mol	Eq. 7*n*
Advancement, *e*	$d_{tr}\zeta_{H+/e}$	$d_{tr}\zeta_{H+/e} = de_{H+} \cdot \nu_{H+}^{-1}$	C	Eq. 7*e*
Electric partial force, *e*	$F_{el/e}$	$F_{el/e} \equiv \Delta\Psi$	V	Eq. 8*e*
Electric partial force, *n*	$F_{el/n}$	$\Delta\Psi \cdot F = 96.5 \cdot \Delta\Psi$	$kJ \cdot mol^{-1}$	Eq. 8*n*
Chemical partial force, *e* at 37 °C	$F_{d,H+/e}$	$\Delta\mu_{H+}/F = -\ln(10) \cdot RT/F \cdot \Delta pH$ $= -0.06 \cdot \Delta pH$	V $J \cdot C^{-1}$	Eq. 9*e*
Chemical partial force, *n* at 37 °C	$F_{d,H+/n}$	$\Delta\mu_{H+} = -\ln(10) \cdot RT \cdot \Delta pH$ $= -5.9 \cdot \Delta pH$	$J \cdot mol^{-1}$ $kJ \cdot mol^{-1}$	Eq. 9*n*

775
776 Eq. 4 to 7: An isomorphic motive entity or transformant, expressed in units x, is defined for any
777 transformation, tr. x=mol or C in proton translocation. For comparison, in a mechanical,
778 vectorial advancement, $d_{me}\boldsymbol{\xi}$ [m], the unit of the *force* is newton, $\boldsymbol{F}_{me}$ [N=J·m^{-1}], and *flow* is
779 the velocity, $\boldsymbol{v}=d_{me}\boldsymbol{\xi}/dt$ [m·s^{-1}], such that the flow·force product yields mechanical power,

P_{me} [W] (Cohen *et al.* 2008). The corresponding *vectorial flux* (flow density per area) is velocity per cross-sectional area [$s^{-1} \cdot m^{-1}$]. The *scalar flux* lacks spatial information in a given volume, such that flux ($m \cdot s^{-1}$ per volume [$s^{-1} \cdot m^{-2}$]) times force yields volume-specific power, P_{Vme} [$W \cdot m^{-3}$].

Eq. 5: $\partial_{tr}G$ [J] is the partial Gibbs energy change in the advancement of transformation tr.

Eq. 6: For x=C, flow is electric current, I_{el} [$A = C \cdot s^{-1}$].

Eq. 7*n*: For a chemical reaction, the advancement of reaction r is $d_r\xi_B = d_r n_B \cdot \nu_B^{-1}$ [mol]. The stoichiometric number is ν_B=-1 or ν_B=1, depending on B being a product or substrate, respectively, in reaction r involving one mole of B. The conjugated *intensive* molar quantity, $F_{r,B} = \partial G/\partial_r\xi_B$ [$J \cdot mol^{-1}$], is the chemical force of reaction or *reaction-motive* force per stoichiometric amount of B. In reaction kinetics, $d_r n_B$ is expressed as a volume-specific quantity, which is the partial contribution to the total concentration change of B, $d_r c_B = d_r n_B/V$ and $dc_B = dn_B/V$, respectively. In open systems with constant volume V, $dc_B = d_r c_B + d_e c_B$, where r indicates the *internal* reaction and e indicates the *external* flux of B into the unit volume of the system. At steady state the concentration does not change, dc_B=0, when $d_r c_B$ is compensated for by the external flux of B, $d_r c_B = -d_e c_B$ (Gnaiger 1993b). Alternatively, dc_B=0 when B is held constant by different coupled reactions in which B acts as a substrate or a product.

Eq. 8*e*: Scalar potential difference across the mitochondrial membrane. In a scalar electric transformation (flux of charge, *i.e.* current, from the matrix space to the intermembrane and extramitochondrial space) the motive force is the difference of charge. The endergonic direction of translocation is defined in **Fig. 2** as $H^+_{in} \rightarrow H^+_{out}$.

Eq. 8*n*: F=96.5 ($kJ \cdot mol^{-1}$)/V.

Eq. 9: Note that the electric partial force is independent of temperature (Eq. 8), but the chemical partial force depends on absolute temperature, T [K].

Eq. 9*e*: RT is the gas constant times absolute temperature. $\ln(10) \cdot RT/F$ = 59.16 and 61.54 mV at 298.15 and 310.15 K (25 and 37 °C), respectively.

Eq. 9*n*: $\ln(10) \cdot RT$ = 5.708 and 5.938 $kJ \cdot mol^{-1}$ at 298.15 and 310.15 K (25 and 37 °C), respectively.

3.2. Forces and flows in physics and irreversible thermodynamics

According to its definition in physics, a potential difference and as such the *protonmotive force*, Δp_{H+}, is not a force *per se* (Cohen *et al.* 2008). The fundamental forces of physics are distinguished from *motive forces* of statistical and irreversible thermodynamics. Complementary to the attempt towards unification of fundamental forces defined in physics, the concepts of Nobel laureates Lars Onsager, Erwin Schrödinger, Ilya Prigogine and Peter Mitchell (even if expressed in apparently unrelated terms) unite the diversity of *generalized* or 'isomorphic' *flow-force* relationships, the product of which links to the dissipation function and Second Law of thermodynamics (Schrödinger 1944; Prigogine 1967). A *motive force* is the derivative of potentially available or 'free' energy (exergy) per isomorphic *motive* unit (**Box 3**). Perhaps the first account of a *motive force* in energy transformation can be traced back to the Peripatetic school around 300 BC in the context of moving a lever, up to Newton's motive force proportional to the alteration of motion (Coopersmith 2010).

Vectorial and scalar forces, and fluxes: In chemical reactions and osmotic or diffusion processes occurring in a closed heterogeneous system, such as a chamber containing isolated mitochondria, scalar transformations occur without measured spatial direction but between separate compartments (translocation between the matrix and intermembrane space) or between energetically-separated chemical substances (reactions from substrates to products). Hence, the corresponding fluxes are not vectorial but scalar, and are expressed per volume and not per membrane area. The corresponding motive forces are also scalar potential *differences* across the membrane (**Table 5**), without taking into account the *gradients* across the 6 nm thick inner mitochondrial membrane (Rich 2003).

Coupling: In energetics (ergodynamics), coupling is defined as an exergy transformation fuelled by an exergonic (downhill) input process driving the advancement of an endergonic (uphill) output process. The (negative) output/input power ratio is the efficiency of a coupled energy transformation (**Box 2**). At the limit of maximum efficiency of a completely coupled

system, the (negative) input power equals the (positive) output power, such that the total power approaches zero at the maximum efficiency of 1, and the process becomes fully reversible without any dissipation of exergy, i.e. without entropy production.

Coupled versus bound processes: Since the chemiosmotic theory describes the mechanisms of coupling in OXPHOS, it may be interesting to ask if the electrical and chemical parts of proton translocation are coupled processes. This is not the case according to the definition of coupling. If the coupling mechanism is disengaged, the output process becomes independent of the input process, and both proceed in their downhill (exergonic) direction (**Fig. 2**). It is not possible to physically uncouple the electrical and chemical processes, which are only *theoretically* partitioned as electrical and chemical components and can be measured separately. If partial processes are non-separable, *i.e.*, cannot be uncoupled, then these are not *coupled* but are defined as *bound* processes. The electrical and chemical parts are tightly bound partial forces of the protonmotive force, since the flow cannot be partitioned but expressed only in either an electrical or chemical isomorphic format (**Table 4**).

4. Normalization: flows and fluxes

4.1. Flux per chamber volume

The volume-specific *flux of a chemical reaction* r is the time derivative of the advancement of the reaction per unit volume, $J_{V,B} = d_r\xi_B/dt \cdot V^{-1}$ [(mol·s^{-1})·L^{-1}]. The *rate of concentration change* is dc_B/dt [(mol·L^{-1})·s^{-1}], where concentration is $c_B = n_B/V$. It is helpful to make the subtle distinction between [mol·s^{-1}·L^{-1}] and [mol·L^{-1}·s^{-1}] for the fundamentally different quantities of volume-specific flux and rate of concentration change, which merge to a single expression only in closed systems. In open systems, external flows (such as O_2 supply) are distinguished from internal transformations (metabolic flow, O_2 consumption). In a closed system, external flows of all substances are zero and O_2 consumption (internal flow), I_{O2} [pmol·s^{-1}], causes a decline of the amount of O_2 in the system, n_{O2} [nmol]. Normalization of

these quantities for the volume of the system, V [L=dm^3], yields volume-specific O_2 flux, $J_{V,O2}=I_{O2}/V$ [nmol·s^{-1}·L^{-1}], and O_2 concentration, [O_2] or $c_{O2} = n_{O2}/V$ [nmol·mL^{-1}=µmol·L^{-1}=µM]. Instrumental background O_2 flux is due to external flux into a non-ideal closed respirometer, such that total volume-specific flux has to be corrected for instrumental background O_2 flux, i.e. O_2 diffusion into or out of the instrumental chamber. $J_{V,O2}$ is relevant mainly for methodological reasons and should be compared with the accuracy of instrumental resolution of background-corrected flux, *e.g.* ±1 nmol·s^{-1}·L^{-1} (Gnaiger 2001). 'Metabolic' indicates O_2 flux corrected for instrumental background O_2 flux and chemical background O_2 flux due to autoxidation of chemical components added to the incubation medium.

4.2. Extensive expressions and size-specific normalization

Application of common and generally defined units is required for direct transfer of reported results into a database. The second [s] is the *SI* unit for the base quantity *time*. It is also the standard time-unit used in solution chemical kinetics. **Table 6** lists some conversion factors to obtain *SI* units. The term *rate* is not sufficiently defined to be useful for a database (**Fig. 7**). The inconsistency of the meanings of rate becomes fully apparent when considering Galileo Galilei's famous principle, that 'bodies of different weight all fall at the same rate (have a constant acceleration)' (Coopersmith 2010).

Extensive quantities: An extensive quantity increases proportionally with system size. The magnitude of an extensive quantity is completely additive for non-interacting subsystems, such as mass or flow expressed per defined system. The magnitude of these quantities depends on the extent or size of the system (Cohen *et al.* 2008).

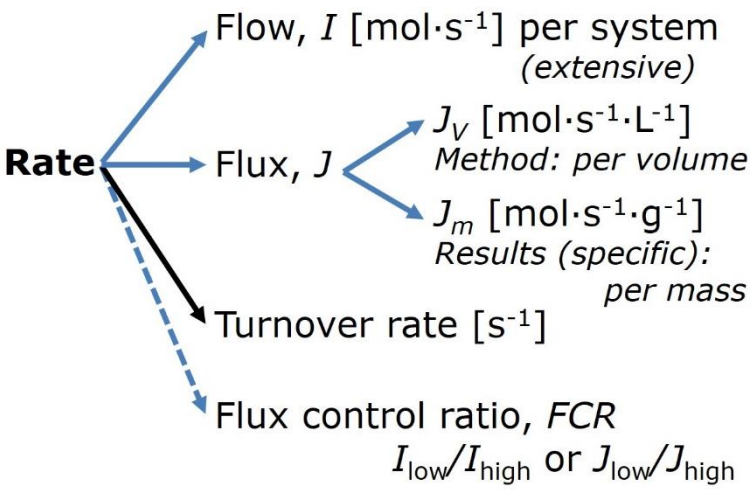

Fig. 7. Different meanings of *rate* may lead to confusion, if the normalization is not sufficiently specified. Results are frequently expressed as mass-specific *flux*, J_m, per mg protein, dry or wet weight (mass). Cell volume, V_{cell}, or mitochondrial volume, V_{mt}, may be used for normalization (volume-specific flux, J_{Vcell} or J_{Vmt}), which then must be clearly distinguished from flux, J_V, expressed for methodological reasons per volume of the measurement system, or flow per cell, I_X.

Size-specific quantities: 'The adjective *specific* before the name of an extensive quantity is often used to mean *divided by mass*' (Cohen *et al.* 2008). Mass-specific flux is flow divided by mass of the system. A mass-specific quantity is independent of the extent of non-interacting homogenous subsystems. Tissue-specific quantities are of fundamental interest in comparative mitochondrial physiology, where *specific* refers to the *type* rather than *mass* of the tissue. The term *specific*, therefore, must be further clarified, such that tissue mass-specific, *e.g.*, muscle mass-specific quantities are defined.

Molar quantities: 'The adjective *molar* before the name of an extensive quantity generally means *divided by amount of substance*' (Cohen *et al.* 2008). The notion that all molar quantities then become *intensive* causes ambiguity in the meaning of *molar Gibbs energy*. It is important to emphasize the fundamental difference between normalization for amount of substance *in a system* or for amount of motive substance *in a transformation*. When the Gibbs energy of a system, G [J], is divided by the amount of substance B in the system, n_B [mol], a *size-specific* molar quantity is obtained, $G_B = G/n_B$ [J·mol^{-1}], which is not any force at all. In contrast, when the partial Gibbs energy change, $\partial_r G$ [J], is divided by the motive amount of substance B in reaction r (advancement of reaction), $\partial_r \xi_B$ [mol], the resulting intensive molar

quantity, $F_{r,B} = \partial G/\partial_r \xi_B$ [J·mol^{-1}], is the chemical motive force of reaction r involving 1 mol B (**Table 5**, Note to Eq. 7).

Flow per system, *I*: In analogy to electrical terms, flow as an extensive quantity (*I*; per system) is distinguished from flux as a size-specific quantity (*J*; per system size) (**Fig. 7**). Electric current is flow, I_{el} [A=C·s^{-1}] per system (extensive quantity). When dividing this extensive quantity by system size (membrane area), a size-specific quantity is obtained, which is electric flux (electric current density), $\boldsymbol{J}_{el}$ [A·m^{-2} = C·s^{-1}·m^{-2}].

Size-specific flux, *J*: Metabolic O_2 flow per tissue increases as tissue mass is increased. Tissue mass-specific O_2 flux should be independent of the size of the tissue sample studied in the instrument chamber, but volume-specific O_2 flux (per volume of the instrument chamber, *V*) should increase in direct proportion to the amount of sample in the chamber. Accurate definition of the experimental system is decisive: whether the experimental chamber is the closed, open, isothermal or non-isothermal *system* with defined volume as part of the measurement apparatus, in contrast to the experimental *sample* in the chamber (**Table 6**). Volume-specific O_2 flux depends on mass-concentration of the sample in the chamber, but should be independent of the chamber volume. There are practical limitations to increasing the mass-concentration of the sample in the chamber, when one is concerned about crowding effects and instrumental time resolution.

Table 6. Sample concentrations and normalization of flux with *SI* base units.

Expression	Symbol	Definition	*SI* Unit	Notes
Sample				
Identity of sample	X	Cells, animals, patients		
Number of sample entities X	N_X	Number of cells, *etc.*	x	
Mass of sample X	m_X		kg	1
Mass of entity X	M_X	$M_X = m_X \cdot N_X^{-1}$	$kg \cdot x^{-1}$	1
Mitochondria				
Mitochondria	mt	X=mt		
Amount of mt-elements	mte	Quantity of mt-marker	x_{mte}	
Concentrations				
Sample number concentration	C_{NX}	$C_{NX} = N_X \cdot V^{-1}$	$x \cdot m^{-3}$	2
Sample mass concentration	C_{mX}	$C_{mX} = m_X \cdot V^{-1}$	$kg \cdot m^{-3}$	
Mitochondrial concentration	C_{mte}	$C_{mte} = mte \cdot V^{-1}$	$x_{mte} \cdot m^{-3}$	3
Specific mitochondrial density	D_{mte}	$D_{mte} = mte \cdot m_X^{-1}$	$x_{mte} \cdot kg^{-1}$	4
Mitochondrial content, mte per entity X	mte_X	$mte_X = mte \cdot N_X^{-1}$	$x_{mte} \cdot x^{-1}$	5
O_2 flow and flux				6
Flow	I_{O2}	Internal flow	$mol \cdot s^{-1}$	7
Volume-specific flux	$J_{V,O2}$	$J_{V,O2} = I_{O2} \cdot V^{-1}$	$mol \cdot s^{-1} \cdot m^{-3}$	8
Flow per sample entity X	$I_{X,O2}$	$I_{X,O2} = J_{V,O2} \cdot C_{NX}^{-1}$	$mol \cdot s^{-1} \cdot x^{-1}$	9
Mass-specific flux	$J_{mX,O2}$	$J_{mX,O2} = J_{V,O2} \cdot C_{mX}^{-1}$	$mol \cdot s^{-1} \cdot kg^{-1}$	
Mitochondria-specific flux	$J_{mte,O2}$	$J_{mte,O2} = J_{V,O2} \cdot C_{mte}^{-1}$	$mol \cdot s^{-1} \cdot x_{mte}^{-1}$	10

1 The *SI* prefix k is used for the SI base unit of mass (kg=1,000 g). In praxis, various *SI* prefixes are used for convenience, to make numbers easily readable, *e.g.* 1 mg tissue, cell or mitochondrial mass instead of 0.000001 kg.

2 In case X=cells, the sample number concentration is $C_{Ncell}=N_{cell} \cdot V^{-1}$, and volume may be expressed in [dm^3=L] or [cm^3=mL]. See Table 7 for different sample types.

3 mt-concentration is an experimental variable, dependent on sample concentration: (*1*) $C_{mte}=mte \cdot V^{-1}$; (*2*) $C_{mte}=mte_X \cdot C_{NX}$; (*3*) $C_{mte}=C_{mX} \cdot D_{mte}$.

4 If the amount of mitochondria, mte, is expressed as mitochondrial mass, then D_{mte} is the mass fraction of mitochondria in the sample. If mte is expressed as mitochondrial volume, V_{mt}, and the mass of sample, m_X, is replaced by volume of sample, V_X, then D_{mte} is the volume fraction of mitochondria in the sample.

5 $mte_X=mte \cdot N_X^{-1}=C_{mte} \cdot C_{NX}^{-1}$.

6 Entity O_2 can be replaced by other chemical entities B to study different reactions.

7 I_{O2} and V are defined per instrument chamber as a system of constant volume (and constant temperature), which may be closed or open. I_{O2} is abbreviated for $I_{r,O2}$, *i.e.* the metabolic or internal O_2 flow of the chemical reaction r in which O_2 is consumed, hence the negative stoichiometric number, ν_{O2}=-1. $I_{r,O2}=d_r n_{O2}/dt\cdot\nu_{O2}^{-1}$. If r includes all chemical reactions in which O_2 participates, then $d_r n_{O2} = dn_{O2} - d_e n_{O2}$, where dn_{O2} is the change in the amount of O_2 in the instrument chamber and $d_e n_{O2}$ is the amount of O_2 added externally to the system. At steady state, by definition $dn_{O2}=0$, hence $d_r n_{O2}=-d_e n_{O2}$.

8 $J_{V,O2}$ is an experimental variable, expressed per volume of the instrument chamber.

9 $I_{X,O2}$ is a physiological variable, depending on the size of entity X.

10 There are many ways to normalize for a mitochondrial marker, that are used in different experimental approaches: (*1*) $J_{mte,O2} = J_{V,O2}\cdot C_{mte}^{-1}$; (*2*) $J_{mte,O2} = J_{V,O2}\cdot C_{mX}^{-1}\cdot D_{mte}^{-1} = J_{mX,O2}\cdot D_{mte}^{-1}$; (*3*) $J_{mte,O2} = J_{V,O2}\cdot C_{NX}^{-1}\cdot mte_X^{-1} = I_{X,O2}\cdot mte_X^{-1}$; (*4*) $J_{mte,O2} = I_{O2}\cdot mte^{-1}$.

Table 7. Some useful abbreviations of various sample types, *X*.

Identity of sample	*X*
Mitochondrial preparations	mtprep
Isolated mitochondria	imt
Tissue homogenate	thom
Permeabilized tissue	pti
Permeabilized fibres	pfi
Permeabilized cells	pce
Cells	ce

Sample concentration C_{mX}: Normalization for sample concentration is required for reporting respiratory data. Consider a tissue or cells as the sample, X, and the sample mass, m_X [mg] from which a mitochondrial preparation is obtained. The sample mass is frequently measured as wet or dry weight ($m_X \equiv W_w$ or W_d [mg]), or as amount of tissue or cell protein

($m_X \equiv m_{Protein}$). In the case of permeabilized tissues, cells, and homogenates, the sample concentration, $C_{mX}=m_X/V$ [mg·mL^{-1}=g·L^{-1}], is simply the mass of the subsample of tissue that is transferred into the instrument chamber. Part of the mitochondria from the tissue is lost during preparation of isolated mitochondria, and only a fraction of mitochondria is obtained, expressed as the mitochondrial yield (**Fig. 8**). At a high mitochondrial yield the sample of isolated mitochondria is more representative of the total mitochondrial population than in preparations characterized by low mitochondrial yield. Determination of the mitochondrial yield is based on measurement of the concentration of a mitochondrial marker in the tissue homogenate, $C_{mte,thom}$, which simulatenously provides information on the specific mitochondrial density in the sample (**Fig. 8**).

Mass-specific flux, $J_{mX,O2}$: Mass-specific flux is obtained by expressing respiration per mass of sample, m_X [mg]. *X* is the type of sample, *e.g.*, tissue homogenate, permeabilized fibres or cells. Volume-specific flux is divided by mass concentration of *X*, $J_{mX,O2} = J_{V,O2}/C_{mX}$; or flow per cell is divided by mass per cell, $J_{mcell,O2} = I_{cell,O2}/M_{cell}$. If mass-specific O_2 flux is constant and independent of sample size (expressed as mass), then there is no interaction between the subsystems. A 1.5 mg and a 3.0 mg muscle sample respires at identical mass-specific flux. Mass-specific O_2 flux, however, may change with the mass of a tissue sample, cells or isolated mitochondria in the measuring chamber, in which case the nature of the interaction becomes an issue. Optimization of cell density and arrangement is generally important and particularly in experiments carried out in wells, considering the confluency of the cell monolayer or clumps of cells (Salabei *et al.* 2014).

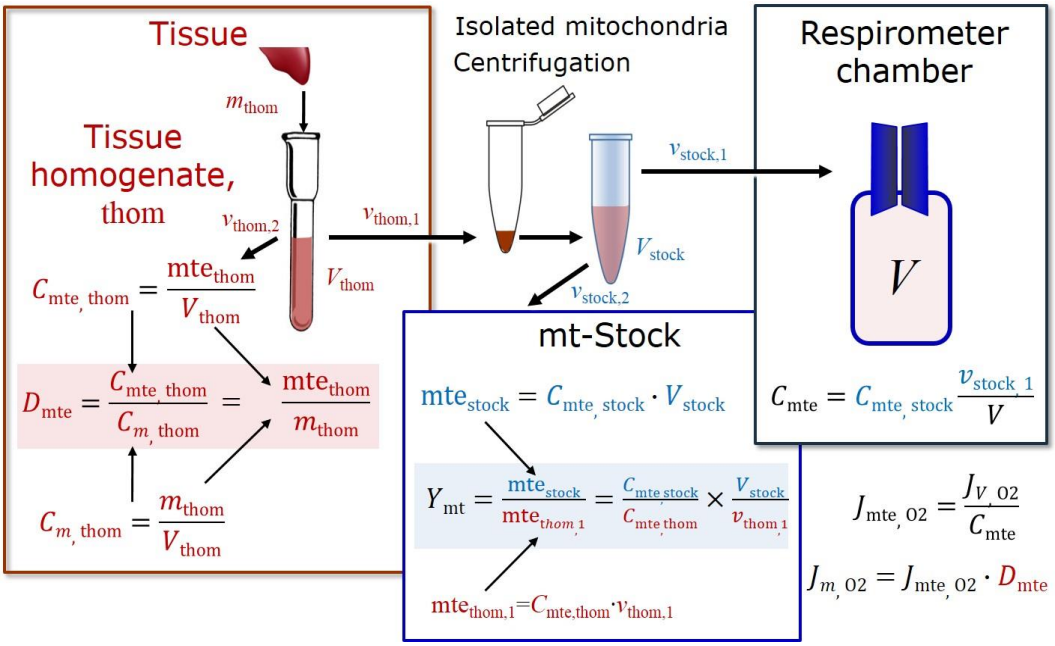

1010

Symbol	Definition [Units]
C_{mte}	Mitochondrial concentration in chamber [$x_{mte} \cdot L^{-1}$]
C_m	Sample mass concentration in chamber [$g \cdot L^{-1}$]
D_{mte}	Specific mte-density per tissue mass [$x_{mte} \cdot g^{-1}$]
$J_{m,O2}$	Mass-specific O_2 flux [$nmol \cdot s^{-1} \cdot g^{-1}$]
$J_{mte,O2}$	Mitochondria-specific O_2 flux [$nmol \cdot s^{-1} \cdot x_{mte}^{-1}$]
mte	Amount of mitochondrial elements [x_{mte}]
m_{thom}	Mass of tissue in the homogenate [g]
Y_{mt}	Yield of isolated mitochondria

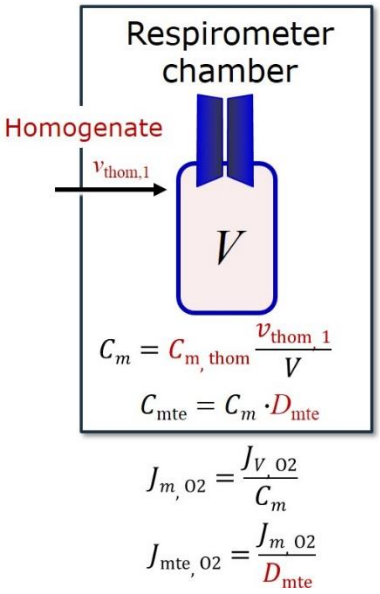

1011

1012 **Fig. 8. Normalization of volume-specific flux of isolated mitochondria and tissue**
1013 **homogenate. A:** Mitochondrial yield, Y_{mt}, in preparation of isolated mitochondria. $v_{thom,1}$
1014 and $v_{stock,1}$ are the volumes transferred from the total volume, V_{thom} and V_{stock}, respectively.
1015 $mte_{thom,1}$ is the amount of mitochondrial elements in volume $v_{thom,1}$ used for isolation. **B:**
1016 In respirometry with homogenate, $v_{thom,1}$ is transferred directly into the respirometer
1017 chamber. See **Table 6** for further explanation of symbols.

1018

Number concentration, C_{NX}: The experimental *number concentration* of sample in the case of cells or animals, *e.g.*, nematodes is $C_{NX}=N_X/V$ [x·mL^{-1}], where N_X is the number of cells or organisms in the chamber (**Table 6**).

Flow per sample entity, $I_{X,O2}$: A special case of normalization is encountered in respiratory studies with permeabilized (or intact) cells. If respiration is expressed per cell, the O_2 flow per measurement system is replaced by the O_2 flow per cell, $I_{cell,O2}$ (**Table 6**). O_2 flow can be calculated from volume-specific O_2 flux, $J_{V,O2}$ [nmol·s^{-1}·L^{-1}] (per V of the measurement chamber [L]), divided by the number concentration of cells, $C_{Nce}=N_{ce}/V$ [cell·L^{-1}], where N_{ce} is the number of cells in the chamber. Cellular O_2 flow can be compared between cells of identical size. To take into account changes and differences in cell size, further normalization is required to obtain cell size-specific or mitochondrial marker-specific O_2 flux (Renner *et al.* 2003).

The complexity changes when the sample is a whole organism studied as an experimental model. The well-established scaling law in respiratory physiology reveals a strong interaction of O_2 consumption and individual body mass of an organism, since *basal* metabolic rate (flow) does not increase linearly with body mass, whereas *maximum* mass-specific O_2 flux, $\dot{V}_{O2max}$ or $\dot{V}_{O2peak}$, is approximately constant across a large range of individual body mass (Weibel and Hoppeler 2005), with individuals, breeds, and certain species deviating substantially from this general relationship. $\dot{V}_{O2peak}$ of human endurance athletes is 60 to 80 mL O_2·min^{-1}·kg^{-1} body mass, converted to $J_{m,O2peak}$ of 45 to 60 nmol·s^{-1}·g^{-1} (Gnaiger 2014; **Table 8**).

4.2. Normalization for mitochondrial content

Normalization is a problematic subject and it is essential to consider the question of the study. If the study aims to compare tissue performance, such as the effects of a certain treatment on a specific tissue, then normalization can be successful, using tissue mass or protein content, for example. If the aim, however, is to find differences of mitochondrial function independent of mitochondrial density (**Table 6**), then normalization to a mitochondrial marker is imperative.

However, one cannot assume that quantitative changes in various markers such as mitochondrial proteins necessarily occur in parallel with one another. It is important to first establish that the marker chosen is not selectively altered by the performed treatment. In conclusion, the normalization must reflect the question under investigation to reach a satisfying answer. On the other hand, the goal of comparing results across projects and institutions requires some standardization on normalization for entry into a databank.

Mitochondrial concentration, C_{mte}, and mitochondrial markers: It is important that mitochondrial content in the tissue and the measurement chamber be quantified, as a physiological output and result of mitochondrial biogenesis and degradation, and as a quantity for normalization in functional analyses. Mitochondrial organelles comprise a cellular reticulum that is in a continual flux of fusion and fission. Hence the definition of an "amount" of mitochondria is often misconceived: mitochondria cannot be counted as a number of occurring elements. Therefore, quantification of the "amount" of mitochondria depends on measurement of chosen mitochondrial markers. ‘Mitochondria are the structural and functional elemental units of cell respiration’ (Gnaiger 2014). The quantity of a mitochondrial marker can be considered as the measurement of the amount of *elemental mitochondrial units* or *mitochondrial elements*, mte. However, since mitochondrial quality changes under certain stimuli, particularly in mitochondrial dysfunction, some markers can vary while other markers are unchanged. (*1*) Mitochondrial volume or membrane area are structural markers, whereas mitochondrial protein mass is frequently used as a marker for isolated mitochondria. (*2*) Mitochondrial marker enzymes (amounts or activities) and molecular markers can be selected as matrix markers, *e.g.*, citrate synthase activity, mtDNA; or inner mt-membrane markers, *e.g.*, cytochrome *c* oxidase activity, aa_3 content, cardiolipin, TOM20. (*3*) Extending the measurement of mitochondrial marker enzyme activity to mitochondrial pathway capacity, measured as ETS or OXPHOS capacity, can be considered as an integrative functional mitochondrial marker.

Depending on the type of mitochondrial marker, the mitochondrial elements, mte, are expressed in marker-specific units. Although concentration and density are used synonymously in physical chemistry, it is recommended to distinguish *experimental mitochondrial concentration*, C_{mte}=mte/V and *physiological mitochondrial density*, D_{mte}= mte/m_X. Then mitochondrial density is the amount of mitochondrial elements per mass of tissue. The former is mitochondrial density multiplied by sample mass concentration, $C_{mte}=D_{mte}\cdot C_{mX}$, or mitochondrial content multiplied by sample number concentration, $C_{mte}=mte_X\cdot C_{NX}$ (**Table 6**).

Mitochondria-specific flux, $J_{mte,O2}$: Volume-specific metabolic O_2 flux depends on: (*1*) the sample concentration in the volume of the instrument chamber, C_{mX}, or C_{NX}; (*2*) the mitochondrial density in the sample, D_{mte}=mte/m_X or mte_X=mte/N_X; and (*3*) the specific mitochondrial activity or performance per elemental mitochondrial unit, $J_{mte,O2}=J_{V,O2}/C_{mte}$ (**Table 6**). Obviously, the numerical results for $J_{mte,O2}$ vary according to the type of mitochondrial marker chosen for measurement of mte and C_{mte}=mte/V. Some problems are common for all mitochondrial markers: (*1*) Accuracy of measurement is crucial, since even a highly accurate and reproducible measurement of O_2 flux becomes inaccurate and noisy if normalized for a biased and noisy measurement of a mitochondrial marker. This problem is acute in mitochondrial respiration because the denominators used (the mitochondrial marker) are often very small moieties whose accurate and precise determination is difficult. This problem can be avoided when O_2 fluxes measured in substrate-uncoupler-inhibitor titration protocols are normalized for flux in a defined respiratory reference state, which is used as an *internal* marker and yields flux control ratios, *FCR*s (**Fig. 7**). *FCR*s are independent of any *externally* measured markers and, therefore, are statistically very robust. *FCR*s indicate qualitative changes of mitochondrial respiratory control, with highest quantitative resolution, separating the effect of mitochondrial density or concentration on $J_{mX,O2}$ or $I_{X,O2}$ from that of function per elemental mitochondrial marker, $J_{mte,O2}$ (Pesta *et al.* 2011; Gnaiger 2014). (*2*) If mitochondrial quality does not change and only the amount of mitochondria, defined by the

chosen mitochondrial marker, varies as a determinant of mass-specific flux, then any marker is equally qualified and selection of the optimum marker depends only on the accuracy and precision of measurement of the mitochondrial marker. (*3*) If mitochondrial flux control ratios change, then there may not be any best mitochondrial marker. In general, measurement of multiple mitochondrial markers enables a comparison and evaluation of normalization for a variety of mitochondrial markers.

4.3. Conversion: oxygen, protons, ATP

Many different units have been used to report the rate of oxygen consumption, OCR (**Tables 8 and 9**). For cellular studies we recommend that respiration be expressed as O_2 flux in units of cell volume or mass, for comparison of respiration of cells with different cell size (Renner *et al.* 2003) and with studies on tissue preparations, and as O_2 flow in units of attomole (10^{-18} mol) of O_2 consumed by each cell in a second [amol·s^{-1}·cell^{-1}], numerically equivalent to [pmol·s^{-1}·10^{-6} cells]. This convention allows information to be easily used when designing experiments in which oxygen consumption must be considered. For example, to estimate the volume-specific O_2 flux in an instrument chamber that would be expected at a particular cell number concentration, one simply needs to multiply the flow per cell by the number of cells per volume of interest. This provides the amount of O_2 [mol] consumed per time [s^{-1}] per unit volume [L^{-1}]. At an O_2 flow of 100 amol·s^{-1}·cell^{-1} and a cell density of 10^9 cells·L^{-1} (10^6 cells·mL^{-1}), the volume-specific O_2 flux is 100 nmol·s^{-1}·L^{-1} (100 pmol·s^{-1}·mL^{-1}). Although volume is expressed as m^3 using the *SI* base unit, the litre [dm^3] is the basic unit of volume for concentration and is used for most solution chemical kinetics. If one multiplies $I_{cell,O2}$ by C_{Ncell}, then the result will not only be the amount of O_2 [mol] consumed per time [s^{-1}] in one litre [L^{-1}], but also the change in the concentration of oxygen per second (for any volume of an ideally closed system). This is ideal for kinetic modeling as it blends with chemical rate equations where concentrations are typically expressed in mol·L^{-1} (Wagner *et al.* 2011). In studies of

multinuclear cells, such as differentiated skeletal muscle cells, it is easy to determine the number of nuclei but not the total number of cells. A generalized concept, therefore, is obtained by substituting cells by nuclei as the sample entity. This does not hold, however, for enucleated platelets which comprise 5% of human cells (Sender *et al.* 2016).

Table 8. Conversion of various units used in respirometry and ergometry. e is the number of electrons or reducing equivalents. z_B is the charge number of entity B.

1 Unit	x	Multiplication factor	*SI*-Unit	Note
ng.atom O·s^{-1}	(2 e)	0.5	nmol O_2·s^{-1}	
ng.atom O·min^{-1}	(2 e)	8.33	pmol O_2·s^{-1}	
natom O·min^{-1}	(2 e)	8.33	pmol O_2·s^{-1}	
nmol O_2·min^{-1}	(4 e)	16.67	pmol O_2·s^{-1}	
nmol O_2·h^{-1}	(4 e)	0.2778	pmol O_2·s^{-1}	
mL O_2·min^{-1} at STPD[a]		0.744	µmol O_2·s^{-1}	1
W = J/s at -470 kJ/mol O_2		-2.128	µmol O_2·s^{-1}	
mA = mC·s^{-1}	(z_{H+}=1)	10.36	nmol H^+·s^{-1}	2
mA = mC·s^{-1}	(z_{O2}=4)	2.59	nmol O_2·s^{-1}	2
nmol H^+·s^{-1}	(z_{H+}=1)	0.09649	mA	3
nmol O_2·s^{-1}	(z_{O2}=4)	0.38594	mA	3

1 At standard temperature and pressure dry (STPD: 0 °C=273.15 K and 1 atm=101.325 kPa=760 mmHg), the molar volume of an ideal gas, V_m, and $V_{m,O2}$ is 22.414 and 22.392 L.mol^{-1} respectively. Rounded to three decimal places, both values yield the conversion factor of 0.744. For comparison at NTPD (20 °C), $V_{m,O2}$ is 24.038 L.mol^{-1}. Note that the *SI* standard pressure is 100 kPa.

2 The multiplication factor is $10^6/(z_B \cdot F)$.

3 The multiplication factor is $z_B \cdot F/10^6$.

Table 9. Conversion for units with preservation of numerical values.

Name	Frequently used unit	Equivalent unit	Note
Volume-specific flux, $J_{V,O2}$	pmol·s^{-1}·mL^{-1}	nmol·s^{-1}·L^{-1}	1
	mmol·s^{-1}·L^{-1}	mol·s^{-1}·m^{-3}	
Cell-specific flow, I_{O2}	pmol·s^{-1}·10^{-6} cells	amol·s^{-1}·cell^{-1}	2
	pmol·s^{-1}·10^{-9} cells	zmol·s^{-1}·cell^{-1}	3
Cell number concentration, C_{Nce}	10^{6} cells·mL^{-1}	10^{9} cells·L^{-1}	
Mitochondrial protein concentration, C_{mte}	0.1 mg·mL^{-1}	0.1 g·L^{-1}	
Mass-specific flux, $J_{m,O2}$	pmol·s^{-1}·mg^{-1}	nmol·s^{-1}·g^{-1}	4
Catabolic power, $P_{k,O2}$	µW·10^{-6} cells	pW·cell^{-1}	1
Volume	1,000 L	m^3 (1,000 kg)	
	L	dm^3 (kg)	
	mL	cm^3 (g)	
	µL	mm^3 (mg)	
	fL	µm^3 (pg)	
Amount of substance concentration	M = mol·L^{-1}	mol·dm^{-3}	

1 pmol: picomole = 10^{-12} mol
2 amol: attomole = 10^{-18} mol
3 zmol: zeptomole = 10^{-21} mol
4 nmol: nanomole = 10^{-9} mol

J_{O2} is coupled in mitochondrial steady states to proton cycling, $J_{\infty H+} = J_{H+out} = J_{H+in}$ (**Fig. 2**). $J_{H+out/n}$ and $J_{H+in/n}$ [nmol·s^{-1}·L^{-1}] are converted into electrical units, $J_{H+out/e}$ [mC·s^{-1}·L^{-1}=mA·L^{-1}] = $J_{H+out/n}$ [nmol·s^{-1}·L^{-1}]·F [C·mol^{-1}]·10^{-6} (**Table 4**). At a J_{H+out}/J_{O2} ratio or H^+_{out}/O_2 of 20 (H^+_{out}/O=10), a volume-specific O_2 flux of 100 nmol·s^{-1}·L^{-1} would correspond to a proton flux of 2,000 nmol H^+_{out}·s^{-1}·L^{-1} or volume-specific current of 193 mA·L^{-1}.

$$J_{V,H+out/e}\ [mA·L^{-1}] = J_{V,H+out/n}·F·10^{-6}\ [nmol·s^{-1}·L^{-1}·mC·nmol^{-1}] \quad \text{(Eq. 10.1)}$$

$$J_{V,H+out/e}\ [mA·L^{-1}] = J_{V,O2}·(H^+_{out}/O_2)·F·10^{-6}\ [mC·s^{-1}·L^{-1}=mA·L^{-1}] \quad \text{(Eq. 10.2)}$$

ETS capacity in various human cell types including HEK 293, primary HUVEC and fibroblasts ranges from 50 to 180 amol·s^{-1}·cell^{-1}, measured in intact cells in the noncoupled state (see Gnaiger 2014). At 100 amol·s^{-1}·cell^{-1} corrected for ROX (corresponding to a catabolic power of -48 pW·cell^{-1}), the current across the mt-membranes, I_e, approximates 193 pA·cell^{-1} or 0.2 nA per cell. See Rich (2003) for an extension of quantitative bioenergetics from the molecular to the human scale, with a transmembrane proton flux equivalent to 520 A in an adult at a

1162 catabolic power of -110 W. Modelling approaches illustrate the link between proton motive
1163 force and currents (Willis *et al.* 2016).

1164 For NADH- and succinate-linked respiration, the mechanistic »P/O_2 ratio (referring to the
1165 full 4 electron reduction of O_2) is calculated at 20/3.7 and 12/3.7, respectively (Eq. 11) equal to
1166 5.4 and 3.3. The classical »P/O ratios (referring to the 2 electron reduction of 0.5 O_2) are 2.7
1167 and 1.6 (Watt *et al.* 2010), in direct agreement with the measured »P/O ratio for succinate of
1168 1.58 ± 0.02 (Gnaiger *et al.* 2000; for detailed reviews see Wikström and Hummer 2012;
1169 Sazanov 2015),

1170 $$»P/O_2 = (H^+_{out}/O_2)/(H^+_{in}/»P) \quad (11)$$

1171 In summary (**Fig. 1**),

1172 $$J_{V,»P}\ [nmol \cdot s^{-1} \cdot L^{-1}] = J_{V,O2} \cdot (H^+_{out}/O_2)/(\ H^+_{in}/»P) \quad (12.1)$$

1173 $$J_{V,»P}\ [nmol \cdot s^{-1} \cdot L^{-1}] = J_{V,O2} \cdot (»P/O_2) \quad (12.2)$$

1174 We consider isolated mitochondria as powerhouses and proton pumps as molecular machines
1175 to relate experimental results to energy metabolism of the intact cell. The cellular »P/O_2 based
1176 on oxidation of glycogen is increased by the glycolytic (fermentative) substrate-level
1177 phosphorylation of 3 »P/Glyc, *i.e.*, 0.5 mol »P for each mol O_2 consumed in the complete
1178 oxidation of a mol glycosyl unit (Glyc). Adding 0.5 to the mitochondrial »P/O_2 ratio of 5.4
1179 yields a bioenergetic cell physiological »P/O_2 ratio close to 6. Two NADH equivalents are
1180 formed during glycolysis and transported from the cytosol into the mitochondrial matrix, either
1181 by the malate-aspartate shuttle or by the glycerophosphate shuttle resulting in different
1182 theoretical yield of ATP generated by mitochondria, the energetic cost of which potentially
1183 must be taken into account. Considering also substrate-level phosphorylation in the TCA cycle,
1184 this high »P/O_2 ratio not only reflects proton translocation and OXPHOS studied in isolation,
1185 but integrates mitochondrial physiology with energy transformation in the living cell (Gnaiger
1186 1993a).

For an overall perspective of mitochondrial physiology, we may link cellular bioenergetics to systemic human respiratory activity, addressing cell- and tissue-specific mitochondrial function as the next step. An O_2 flow of 234 μmol·s^{-1} per individual or flux of 3.3 nmol·s^{-1}·g^{-1} body mass corresponds to -110 W catabolic energy flow at a body mass of 70 kg and -470 kJ/mol O_2. Considering a cell count of 514·10^6 to 646·10^6 cells per g cell mass (Sender *et al.* 2016; Ahluwalia 2017), the average O_2 flow per cell at $J_{m,O2peak}$ of 45 nmol·s^{-1}·g^{-1} (60 mL O_2·min^{-1}·kg^{-1}) is 88 amol·s^{-1}·cell^{-1}, which compares well with OXPHOS capacity of human fibroblasts (Gnaiger 2014). We can describe our bodies as the sum of 30·10^{12} human cells (30 trillion) and 38·10^{12} microbial cells; Sender *et al.* 2016). At 5 L of blood and 5·10^{12} erythrocytes/L, the number of red blood cells not containing mitochondria is 25·10^{12} or 84% compared to the total number of mitochondria-containing cells of 6·10^{12} (Sender *et al.* 2016). An estimate of mitochondrial content at 300 mitochondria per cell (West *et al.* 2002) raises questions on the concept of mitochondrial 'number' (90-680 per cell; Robin and Wong 1988). Cell count is controversial in the case of multinuclear muscle cells, which contribute 43% to the total cell mass of a reference man of 70 kg total body mass. Subtracting 25% extracellular fluid and 7% extracellular solids, a cell mass of 46 kg is obtained, of which 20 kg is myocytes and 13 kg is adipocytes. If the total number of mitochondria is 2·10^{15} (2 quadrillion mt or 300 mitochondria x 6·10^{12} of cells containing mitochondria), mitochondrial fitness is indicated if O_2 flow of 0.1 amol·s^{-1}·mt^{-1} at rest can be activated to 1.7 amol·s^{-1}·mt^{-1} at high ergometric performance. {*EG: These numbers must be re-examined, on the basis of nuclei per muscle cells mass. Please, consider these figures as they are now merely as an illustration of the rationale, not as final calculations at all. Any critical input is highly welcome.*}

5. Conclusions

MitoEAGLE can serve as a gateway to better diagnose mitochondrial respiratory defects linked to genetic variation, age-related health risks, sex-specific mitochondrial performance,

lifestyle with its effects on degenerative diseases, and thermal and chemical environment. The present recommendations on coupling control states and rates, linked to the concept of the protonmotive force (Part 1) will be extended in a series of manuscripts on pathway control of mitochondrial respiration, respiratory states in intact cells, and harmonization of experimental procedures.

The optimal choice for expressing O_2 flow per biological system, and normalization for specific tissue-markers (volume, mass, protein) and mitochondrial markers (volume, protein, content, mtDNA, activity of marker enzymes, respiratory reference state) is guided by the scientific question. Interpretation of the obtained data depends critically on appropriate normalization, and therefore reporting rates merely as $nmol \cdot s^{-1}$ is discouraged, since it restricts the analysis to intra-experimental comparison of relative (qualitative) differences. Expressing O_2 consumption per cell may not be possible when dealing with tissues. For studies with mitochondrial preparations, we recommend that normalizations be provided as far as possible: (*1*) on a per cell basis as O_2 flow (a biophysical normalization); (*2*) per g cell or tissue protein, or per cell or tissue mass as mass-specific O_2 flux (a cellular normalization); and (*3*) per mitochondrial marker as mt-specific flux (a mitochondrial normalization). With information on cell size and the use of multiple normalizations, maximum potential information is available (Renner *et al.* 2003; Wagner *et al.* 2011; Gnaiger 2014). When using isolated mitochondria, mitochondrial protein is a frequently applied mitochondrial marker, the use of which is basically restricted to isolated mitochondria. Mitochondrial markers, such as citrate synthase activity as an enzymatic matrix marker, provide a link to the tissue of origin on the basis of calculating the mitochondrial yield, *i.e.*, the fraction of mitochondrial marker obtained from a unit mass of tissue.

Acknowledgements

We thank M. Beno for management assistance. Supported by COST Action CA15203 MitoEAGLE and K-Regio project MitoFit (EG).

Competing financial interests: E.G. is founder and CEO of Oroboros Instruments, Innsbruck, Austria.

6. References (*incomplete; www links will be deleted in the final version*)

Ahluwalia A. Allometric scaling in-vitro. Sci Rep 2017;7:42113.

Altmann R. Die Elementarorganismen und ihre Beziehungen zu den Zellen. Zweite vermehrte Auflage. Verlag Von Veit & Comp, Leipzig 1894;160 pp. - www.mitoeagle.org/index.php/Altmann_1894_Verlag_Von_Veit_%26_Comp

Birkedal R, Laasmaa M, Vendelin M. The location of energetic compartments affects energetic communication in cardiomyocytes. Front Physiol 2014;5:376. doi: 10.3389/fphys.2014.00376. eCollection 2014. PMID: 25324784

Brown GC. Control of respiration and ATP synthesis in mammalian mitochondria and cells. Biochem J 1992;284:1-13. - www.mitoeagle.org/index.php/Brown_1992_Biochem_J

Chance B, Williams GR. Respiratory enzymes in oxidative phosphorylation: III. The steady state. J Biol Chem 1955;217:409-27. - www.mitoeagle.org/index.php/Chance_1955_J_Biol_Chem-III

Chance B, Williams GR. Respiratory enzymes in oxidative phosphorylation. IV. The respiratory chain. J Biol Chem 1955;217:429-38. - www.mitoeagle.org/index.php/Chance_1955_J_Biol_Chem-IV

Chance B, Williams GR. The respiratory chain and oxidative phosphorylation. Adv Enzymol Relat Subj Biochem 1956;17:65-134. - www.mitoeagle.org/index.php/Chance_1956_Adv_Enzymol_Relat_Subj_Biochem

Cohen ER, Cvitas T, Frey JG, Holmström B, Kuchitsu K, Marquardt R, Mills I, Pavese F, Quack M, Stohner J, Strauss HL, Takami M, Thor HL. Quantities, Units and Symbols in Physical Chemistry, IUPAC Green Book 2008;3rd Edition, 2nd Printing, IUPAC & RSC Publishing, Cambridge. - www.mitoeagle.org/index.php/Cohen_2008_IUPAC_Green_Book

Coopersmith J. Energy, the subtle concept. The discovery of Feynman's blocks from Leibnitz to Einstein. Oxford University Press 2010;400 pp.

Dai Q, Shah AA, Garde RV, Yonish BA, Zhang L, Medvitz NA, Miller SE, Hansen EL, Dunn CN, Price TM. A truncated progesterone receptor (PR-M) localizes to the mitochondrion and controls cellular respiration. ???

Dufour S, Rousse N, Canioni P, Diolez P. Top-down control analysis of temperature effect on oxidative phosphorylation. Biochem J 1996;314:743-51.

Ernster L, Schatz G Mitochondria: a historical review. J Cell Biol 1981;91:227s-55s. - www.mitoeagle.org/index.php/Ernster_1981_J_Cell_Biol

Estabrook RW. Mitochondrial respiratory control and the polarographic measurement of ADP:O ratios. Methods Enzymol 1967;10:41-7. - www.mitoeagle.org/index.php/Estabrook_1967_Methods_Enzymol

Fell D. Understanding the control of metabolism. Portland Press 1997.

Garlid KD, Semrad C, Zinchenko V. Does redox slip contribute significantly to mitochondrial respiration? In: Schuster S, Rigoulet M, Ouhabi R, Mazat J-P (eds) Modern trends in biothermokinetics. Plenum Press, New York, London 1993;287-93.

Gerö D, Szabo C. Glucocorticoids suppress mitochondrial oxidant production via upregulation of uncoupling protein 2 in hyperglycemic endothelial cells. PLoS One 2016;11:e0154813.

Gnaiger E. Efficiency and power strategies under hypoxia. Is low efficiency at high glycolytic ATP production a paradox? In: Surviving Hypoxia: Mechanisms of Control and

Adaptation. Hochachka PW, Lutz PL, Sick T, Rosenthal M, Van den Thillart G (eds.) CRC Press, Boca Raton, Ann Arbor, London, Tokyo 1993a:77-109. - www.mitoeagle.org/index.php/Gnaiger_1993_Hypoxia

Gnaiger E. Nonequilibrium thermodynamics of energy transformations. Pure Appl Chem 1993b;65:1983-2002. - www.mitoeagle.org/index.php/Gnaiger_1993_Pure_Appl_Chem

Gnaiger E. Bioenergetics at low oxygen: dependence of respiration and phosphorylation on oxygen and adenosine diphosphate supply. Respir Physiol 2001;128:277-97. - www.mitoeagle.org/index.php/Gnaiger_2001_Respir_Physiol

Gnaiger E. Mitochondrial pathways and respiratory control. An introduction to OXPHOS analysis. 4th ed. Mitochondr Physiol Network 2014;19.12. Oroboros MiPNet Publications, Innsbruck:80 pp. - www.mitoeagle.org/index.php/Gnaiger_2014_MitoPathways

Gnaiger E. Capacity of oxidative phosphorylation in human skeletal muscle. New perspectives of mitochondrial physiology. Int J Biochem Cell Biol 2009;41:1837-45. - www.mitoeagle.org/index.php/Gnaiger_2009_Int_J_Biochem_Cell_Biol

Gnaiger E, Méndez G, Hand SC. High phosphorylation efficiency and depression of uncoupled respiration in mitochondria under hypoxia. Proc Natl Acad Sci USA 2000;97:11080-5. - www.mitoeagle.org/index.php/Gnaiger_2000_Proc_Natl_Acad_Sci_U_S_A

Hofstadter DR. Gödel, Escher, Bach: An eternal golden braid. A metaphorical fugue on minds and machines in the spirit of Lewis Carroll. Harvester Press 1979;499 pp. - www.mitoeagle.org/index.php/Hofstadter_1979_Harvester_Press

Illaste A, Laasmaa M, Peterson P, Vendelin M. Analysis of molecular movement reveals latticelike obstructions to diffusion in heart muscle cells. Biophys J 2012;102:739-48. - PMID: 22385844

Jepihhina N, Beraud N, Sepp M, Birkedal R, Vendelin M. Permeabilized rat cardiomyocyte response demonstrates intracellular origin of diffusion obstacles. Biophys J 2011;101:2112-21. - PMID: 22067148

Komlódi T, Tretter L. Methylene blue stimulates substrate-level phosphorylation catalysed by succinyl-CoA ligase in the citric acid cycle. Neuropharmacology 2017;123:287-98. - www.mitoeagle.org/index.php/Komlodi_2017_Neuropharmacology

Lee SR, Kim HK, Song IS, Youm J, Dizon LA, Jeong SH, Ko TH, Heo HJ, Ko KS, Rhee BD, Kim N, Han J. Glucocorticoids and their receptors: insights into specific roles in mitochondria. Prog Biophys Mol Biol 2013;112:44-54.

Lemieux H, Blier PU, Gnaiger E. Remodeling pathway control of mitochondrial respiratory capacity by temperature in mouse heart: electron flow through the Q-junction in permeabilized fibers. Sci Rep 2017;7:2840. - www.mitoeagle.org/index.php/Lemieux_2017_Sci_Rep

Lenaz G, Tioli G, Falasca AI, Genova ML. Respiratory supercomplexes in mitochondria. In: Mechanisms of primary energy trasduction in biology. M Wikstrom (ed) Royal Society of Chemistry Publishing, London, UK 2017:296-337 (in press)

Margulis L. Origin of eukaryotic cells. New Haven: Yale University Press 1970.

Meinild Lundby AK, Jacobs RA, Gehrig S, de Leur J, Hauser M, Bonne TC, Flück D, Dandanell S, Kirk N, Kaech A, Ziegler U, Larsen S, Lundby C. Exercise training increases skeletal muscle mitochondrial volume density by enlargement of existing mitochondria and not de novo biogenesis. Acta Physiol (Oxf) 2017;[Epub ahead of print].

Miller GA. The science of words. Scientific American Library New York 1991;276 pp. - www.mitoeagle.org/index.php/Miller_1991_Scientific_American_Library

Mitchell P. Chemiosmotic coupling in oxidative and photosynthetic phosphorylation Biochim Biophys Acta Bioenergetics 2011;1807:1507-38. - http://www.sciencedirect.com/science/article/pii/S0005272811002283

Mitchell P, Moyle J. Respiration-driven proton translocation in rat liver mitochondria. Biochem J 1967;105:1147-62. - www.mitoeagle.org/index.php/Mitchell_1967_Biochem_J

Moreno M, Giacco A, Di Munno C, Goglia F. Direct and rapid effects of 3,5-diiodo-L-thyronine (T2). Mol Cell Endocrinol 2017;7207:30092-8.

Morrow RM, Picard M, Derbeneva O, Leipzig J, McManus MJ, Gouspillou G, Barbat-Artigas S, Dos Santos C, Hepple RT, Murdock DG, Wallace DC. Mitochondrial energy deficiency leads to hyperproliferation of skeletal muscle mitochondria and enhanced insulin sensitivity. Proc Natl Acad Sci U S A 2017;114:2705-10. - www.mitoeagle.org/index.php/Morrow_2017_Proc_Natl_Acad_Sci_U_S_A

Nicholls DG, Ferguson S. Bioenergetics 4. Elsevier 2013.

Paradies G, Paradies V, De Benedictis V, Ruggiero FM, Petrosillo G. Functional role of cardiolipin in mitochondrial bioenergetics. Biochim Biophys Acta 2014;1837:408-17. - http://www.mitoeagle.org/index.php/Paradies_2014_Biochim_Biophys_Acta

Price TM, Dai Q. The Role of a Mitochondrial Progesterone Receptor (PR-M) in Progesterone Action. Semin Reprod Med. 2015;33:185-94.

Prigogine I. Introduction to thermodynamics of irreversible processes. Interscience, New York, 1967;3rd ed.

Puchowicz MA, Varnes ME, Cohen BH, Friedman NR, Kerr DS, Hoppel CL. Oxidative phosphorylation analysis: assessing the integrated functional activity of human skeletal muscle mitochondria – case studies. Mitochondrion 2004;4:377-85. - www.mitoeagle.org/index.php/Puchowicz_2004_Mitochondrion

P. M. Quiros, A. Mottis, and J. Auwerx. Mitonuclear communication in homeostasis and stress. Nat Rev Mol Cell Biol 2016;17:213-26.

Renner K, Amberger A, Konwalinka G, Gnaiger E. Changes of mitochondrial respiration, mitochondrial content and cell size after induction of apoptosis in leukemia cells. Biochim Biophys Acta 2003;1642:115-23. - www.mitoeagle.org/index.php/Renner_2003_Biochim_Biophys_Acta

Rich P. Chemiosmotic coupling: The cost of living. Nature 2003;421:583. - www.mitoeagle.org/index.php/Rich_2003_Nature

Robin ED, Wong R. Mitochondrial DNA molecules and virtual number of mitochondria per cell in mammalian cells. J Cell Physiol 1988;136:507-13.

Rostovtseva TK, Sheldon KL, Hassanzadeh E, Monge C, Saks V, Bezrukov SM, Sackett DL. Tubulin binding blocks mitochondrial voltage-dependent anion channel and regulates respiration. Proc Natl Acad Sci USA 2008;105:18746-51. - www.mitoeagle.org/index.php/Rostovtseva_2008_Proc_Natl_Acad_Sci_U_S_A

Rustin P, Parfait B, Chretien D, Bourgeron T, Djouadi F, Bastin J, Rötig A, Munnich A. Fluxes of nicotinamide adenine dinucleotides through mitochondrial membranes in human cultured cells. J Biol Chem 1996;271:14785-90.

Saks VA, Veksler VI, Kuznetsov AV, Kay L, Sikk P, Tiivel T, Tranqui L, Olivares J, Winkler K, Wiedemann F, Kunz WS. Permeabilised cell and skinned fiber techniques in studies of mitochondrial function in vivo. Mol Cell Biochem 1998;184:81-100. - http://www.mitoeagle.org/index.php/Saks_1998_Mol_Cell_Biochem

Salabei JK, Gibb AA, Hill BG. Comprehensive measurement of respiratory activity in permeabilized cells using extracellular flux analysis. Nat Protoc 2014;9:421-38.

Sazanov LA. A giant molecular proton pump: structure and mechanism of respiratory complex I. Nat Rev Mol Cell Biol 2015;16:375-88. - www.mitoeagle.org/index.php/Sazanov_2015_Nat_Rev_Mol_Cell_Biol

Schönfeld P, Dymkowska D, Wojtczak L. Acyl-CoA-induced generation of reactive oxygen species in mitochondrial preparations is due to the presence of peroxisomes. Free Radic Biol Med 2009;47:503-9.

Schrödinger E. What is life? The physical aspect of the living cell. Cambridge Univ Press, 1944. - www.mitoeagle.org/index.php/Gnaiger_1994_BTK

Sender R, Fuchs S, Milo R. Revised estimates for the number of human and bacteria cells in the body. PLoS Biol 2016;14:e1002533.

Simson P, Jepihhina N, Laasmaa M, Peterson P, Birkedal R, Vendelin M. Restricted ADP movement in cardiomyocytes: Cytosolic diffusion obstacles are complemented with a small number of open mitochondrial voltage-dependent anion channels. J Mol Cell Cardiol 2016;97:197-203. - PMID: 27261153

Stucki JW, Ineichen EA. Energy dissipation by calcium recycling and the efficiency of calcium transport in rat-liver mitochondria. Eur J Biochem 1974;48:365-75.

Wagner BA, Venkataraman S, Buettner GR. The rate of oxygen utilization by cells. Free Radic Biol Med. 2011:51:700-712. http://dx.doi.org/10.1016/j.freeradbiomed.2011.05.024 PMCID: PMC3147247

Watt IN, Montgomery MG, Runswick MJ, Leslie AG, Walker JE. Bioenergetic cost of making an adenosine triphosphate molecule in animal mitochondria. Proc Natl Acad Sci U S A 2010;107:16823-7. - www.mitoeagle.org/index.php/Watt_2010_Proc_Natl_Acad_Sci_U_S_A

Weibel ER, Hoppeler H. Exercise-induced maximal metabolic rate scales with muscle aerobic capacity. J Exp Biol 2005;208:1635–44.

West GB, Woodruff WH, Brown JH. Allometric scaling of metabolic rate from molecules and mitochondria to cells and mammals. Proc Natl Acad Sci USA 2002;99 Suppl 1:2473–8.

1414 Wikström M, Hummer G. Stoichiometry of proton translocation by respiratory complex I and
1415 its mechanistic implications. Proc Natl Acad Sci U S A 2012;109:4431-6. -
1416 www.mitoeagle.org/index.php/Wikstroem_2012_Proc_Natl_Acad_Sci_U_S_A
1417 Willis WT, Jackman MR, Messer JI, Kuzmiak-Glancy S, Glancy B. A simple hydraulic
1418 analog model of oxidative phosphorylation. Med Sci Sports Exerc. 2016;48:990-1000.
1419

Supplement

Table S1. SI prefixes (IUPAC).

Submultiple	Prefix	Symbol	Multiple	Prefix	Symbol
10^{-3}	milli	m	10^{3}	kilo	k
10^{-6}	micro	µ	10^{6}	mega	M
10^{-9}	nano	n	10^{9}	giga	G
10^{-12}	pico	p	10^{12}	tera	T
10^{-15}	femto	f	10^{15}	peta	P
10^{-18}	atto	a	10^{18}	exa	E
10^{-21}	zepto	z	10^{21}	zetta	Z